72-3454

WOMACK, William Carl, 1930-
THE DYNAMICS OF SOUNDING ROCKETS AT BURNOUT.

The University of Oklahoma, Ph.D., 1971
Engineering, mechanical

University Microfilms, A XEROX Company, Ann Arbor, Michigan

THIS DISSERTATION HAS BEEN MICROFILMED EXACTLY AS RECEIVED

Downloaded from SHAREOK. Persistent Handle URL: https://hdl.handle.net/11244/3166

THE UNIVERSITY OF OKLAHOMA

THE GRADUATE COLLEGE

THE DYNAMICS OF SOUNDING ROCKETS AT BURNOUT

A DISSERTATION

SUBMITTED TO THE GRADUATE FACULTY

in partial fulfillment of the requirements for the

degree of

DOCTOR OF PHILOSOPHY

BY

WILLIAM CARL WOMACK

Norman, Oklahoma

1971

THE DYNAMICS OF SOUNDING ROCKETS

AT BURNOUT

APPROVED BY

Charles W. Bert

M. Rasmussen

J. A. Payne

D M Egle

S. B. Ellison

DISSERTATION COMMITTEE

PLEASE NOTE:

Some Pages have indistinct print. Filmed as received.

UNIVERSITY MICROFILMS

ACKNOWLEDGMENT

This dissertation is the result of analysis and investigation performed for the University of Oklahoma, the School of Aerospace, Mechanical and Nuclear Engineering of which Dr. T. J. Love is the Director. I express my appreciation to the members of my doctoral committee, Dr. C. W. Bert, Dr. M. L. Rasmussen, Dr. D. M. Egle, Dr. J. A. Payne and Dr. S. B. Eliason.

I would like to thank the many friends who have given me their advice and help during this project. I am particularly indebted to Dr. Bert for serving as chairman of my doctoral committee and for his overall direction of my dissertation effort. I owe a special note of thanks to Dr. F. J. Perdreauville who served as my on-the-spot advisor during this investigation. The manuscript was typed by Mrs. Fiona Duncan.

Finally, I dedicate this work to my wife, Betty Faye, and children, Linda and Kathleen, whose continual encouragement, patience and sacrifice made this possible.

TABLE OF CONTENTS

page

LIST OF TABLES vi

LIST OF FIGURES vii

LIST OF SYMBOLS x

Chapter

I. INTRODUCTION 1

II. THE GENERAL PROBLEM AREA 3

2.1 General 3

2.2 Aeroelastic Divergence 4

2.3 Oscillatory Problems 6

III. THE PRESENT STATE-OF-THE-ART 7

3.1 Structural Coupling Approach 7

3.2 Influence Coefficient Matrix Approach 8

3.3 Critical Load Approach 9

IV. DEVELOPMENT OF THE METHOD 10

4.1 Analytical Philosophy 10

4.2 The Basic Assumptions 13

4.3 The Coordinate System 13

4.4 The Equations of Motions 15

Page

V. APPLICATION OF THE METHOD

5.1 Introduction 21

5.2 The Approach 22

5.3 System Description 24

5.4 Formulation of the Problem 28

VI. DISCUSSION OF RESULTS 34

VII. CLOSURE 44

REFERENCES 46

Appendices

A. DERIVATION OF THE EQUATIONS OF MOTION . . 49

B. TRANSFORMATION OF EQUATIONS INTO AERO-BALLISTIC REFERENCE SYSTEM 70

C. CALCULATION OF THE APPLIED LOADS AND MOMENTS 72

D. THE AEROELASTIC PROGRAM 81

E. THE SHOCK CODE 99

F. THE ANALOG COMPUTER CIRCUIT 101

LIST OF TABLES

Table		Page
1	Typical Nitehawk 9 Trajectory	29
2	Values For Function $f_1(t)$	73

LIST OF FIGURES

Figure		Page
1	The Coordinate System	14
2	The Force System	17
3	The Kinematic System	18
4	The Aeroballistic Reference System	23
5	Technical Data Relative to the TE-416 (Tomahawk) Motor	24
6	The Nitehawk 9	25
7	Weight Distribution for Tomahawk Motor and 9 Inch Payload	26
8	EI Distribution for Tomahawk Motor and 9 Inch Payload .	27
9	The Roll Rate vs. Time	31
10	Function $f_1(t)$ vs. Time	32
11	Function $f_2(t)$ vs. Time	33
12	Yaw Gyro Traces from Tomahawk Flights Showing Normal, Locked-In, and Coning Motion	35
13	Simulated Yaw Data	36/38
14	The Aerodynamic Load	74
15	Elastic Vibration	78,

Figure Page

16 Vibration with Loose Joint 80

17 The Analog Computer Circuit 102

Filmed as received

without page(s) ix .

UNIVERSITY MICROFILMS.

LIST OF SYMBOLS

A	Cross-sectional area
$\bar{A}_x$, $\bar{A}_y$, $\bar{A}_z$	Acceleration of the mass center
C_o, C_o, k_o	Coefficients for rigid body displacements
c_l, C_l, k_l	Coefficients for rigid body rotation
C_{m_q}	Damping coefficient
D	Drag force
EI	Structural rigidity
F_x^*, F_y^*, F_z^*	Aerodynamic forces in x, y, and z directions
$f_1(t)$	Coefficient for restoring moment
$f_2(t)$	Coefficient for damping moment
$f_4(t)$, $f_5(t)$	Coefficient for vibrational moment
I_{xx}, I_{yy}, I_{zz}	Moments of inertia
i, j, k	Unit vector for moving axes
J_{D_y}, J_{D_x}	Jet damping forces
K, AG	Shearing stiffness
ℓ_1, ℓ_2	Missile length to center of mass
M	Total mass
$M_{\theta r}^*$	Aerodynamic moment about center of mass

$M_{r_1}^*, M_{r_2}^*, M_{r_3}^*$	Total moment about center of mass in aeroballistic axes
M_B	Moment due to bent payload
$\dot{m}$	Mass flow rate
$\overline{P}$	Position vector to arbitrary point
P_{xy}, P_{xz}	Aerodynamic force per unit length
$\overline{q}$	Dynamic pressure
q_i, q_j, q_k	Generalized coordinates
$\overline{R}$	Position vector to center of mass
r_1, r_2, r_3	Coordinates in aeroballistic axes
T^*	Motor thrust
T_L	Kinetic energy due to velocity
T_R	Kinetic energy due to rotation
T_T	Total kinetic energy
u_1, u_2, u_3	Deformations of missile axes relative to moving axes
u'_{2T}, u'_{3T}	Slope of displacement at tail
V	Total velocity vector
V_o	Velocity of center of mass
X, Y, Z	Coordinates of fixed axes
x, y, z	Coordinates of moving axes
X_p	Distance from center of mass to particle
α	Total pitch angle
$\overline{\alpha}$	Pitch angle in aeroballistic axes

β	Total yaw angle
$\bar{\beta}$	Yaw angle in aeroballistic axes
γ	Inclination of velocity tangent to vertical
η	Inclination of x axis from vertical
$\theta_1, \theta_2, \theta_3$	Rotation of missile axes
$\bar{\rho}$	Position vector in moving axes
ϕ_i, τ_j, σ_k	Eigenfunctions of a free-free beam
ψ_k, λ_j	Eigenfunctions for bending modes
Ψ , Λ	Angle of rotation relative to moving axes of a transverse slice of the missile
ω	Circular frequency of the ith mode

THE DYNAMICS OF SOUNDING ROCKETS AT BURNOUT

CHAPTER I

INTRODUCTION

"Sounding rockets" are rocket missile systems that are designed for the express purpose of carrying scientific instruments through or above the sensible atmosphere. Until about 1955, sounding rockets were generally staged together using surplus military rockets, some ballistic and airplane technology and lots of faith. For this reason, many sounding rockets have been launched (some successfully and some disastrously) that could hardly qualify as having been designed. The need for reliable sounding rockets was greatly increased by the advent of the Space Age. (If man was to explore space, he must know more about the environment that lies between him and space.) However, this need came at a time when support such as wind tunnel facilities, computer sciences and computational methods were inadequate. The sounding rocket developers at that time borrowed some direction from several engineering fields, mixed nomenclature at will, and used

lots of cut-and-try methods to develop a very strong "rule-of-thumb" technology. This technology is still an ever-present element in nearly all sounding rocket discussions. In its defense, it must be noted that it works beautifully for systems that can be considered rigid bodies.

The nuclear atmospheric testing of the 1950's and the early 1960's uncovered many deficiencies in almost every field of scientific endeavor. The need for better performing, more reliable and less expensive sounding rockets was more apparent. Further impetus was added when our scientists learned that there was no suitable rocket system available for obtaining solar background data during the IQSY (International Quiet Sun Year). Several government agencies, private companies and a few foreign countries attempted to develop systems that would meet one or all of these requirements. As a result of this effort, several satisfactory sounding rocket systems have been developed. The new systems rate high in performance and reliability and are relatively low in cost. They are at least an order of magnitude more sophisticated than their predecessors and for that reason, they are at times called "high-altitude diagnostic rocket systems".

CHAPTER II

THE GENERAL PROBLEM AREAS

2.1 General

The development of the new systems brought with it many new and interesting, but difficult problems. In the older rocket systems, the motors usually had a mass fraction of less than 50%. In the newer systems, the mass fraction may exceed 80%. This was an obvious way to improve the systems' performance but it was this approach that uncovered the need for a "new" technology. The new rocket motors had good structural integrity but they did not satisfy the "rigid body" assumption. Now the "rule-of-thumb" approach was simply inadequate for most cases. The higher performance caused many new problems, a few of which were:

1. Extremely high aerodynamic heating rates.
2. Badly misbehaved laminar/turbulent boundary layer transition points.
3. Antenna shadowing and heating problems.
4. Nonlinear aerodynamics such as nonlinear magnus moments and lee-side vortices.

5. Severe acceleration and vibration environment.

These problems are mentioned only in passing since it is the purpose of this dissertation to address itself to the motion of a flexible missile during and shortly after burnout.

In the past few years, there has been a great deal of work done on the effects of the elastic nature of sounding rocket systems. The elastic structure and the aerodynamic excitation forces may interact to produce a nonoscillatory divergence or several types of oscillatory problems. A brief discussion of some of these problems and the work being done toward their solution seems appropriate at this point.

2.2 Aeroelastic Divergence

Most of the work on aeroelastic effects for rockets has been devoted to aeroelastic divergence. This aeroelastic phenomenon usually results in catastrophic structural failure and nothing in the rocket business gets more attention than a system coming apart at Mach 8.

Under high aerodynamic load, the elastic structure will deflect in accordance with its elastic constraints. This deflection may then introduce greater aerodynamic loads which, in turn, cause even greater deflections, and so on. In a successful rocket flight, an equilibrium is reached between the aerodynamic and elastic forces. If an equilibrium is not established, the structure

will fail and divergence is said to have taken place. This phenomenon may be treated as a static aeroelastic problem wherein time does not appear as an independent variable. Most investigators of this type of problem use a computer iteration procedure similar to that used by Thomson (Ref. 1).

The problem of a dynamic aeroelastic instability or flutter is not a problem that is commonly encountered in sounding rocket design; however, it is a problem that is common to aircraft and to larger missiles. It is characterized by the interplay of aerodynamic, elastic and inertia forces. This interplay at velocities above a "critical flutter speed" will result in an oscillation that is self-sustained; i.e., no external oscillator or forcing mechanism is required. With further increase in velocity, the amplitude of oscillation increases. At velocities well above the critical, a small accidental disturbance of an airfoil can trigger an oscillation of great violence and may destroy the airfoil. A great deal has been written about the flutter phenomenon and Fung has an excellent treatment of flutter in his aeroelasticity book (Ref. 18).

Another phenomenon that closely resembles aeroelastic divergence arises because the structural deflection alters the aerodynamic characteristics of the system in such a manner as to adversely affect the static stability of the system, i.e., the center of pressure may be too near the center of gravity. A perturbation

of the system may then cause catastrophic structural failure. This phenomenon has not received the attention that has been given aeroelastic divergence, but Reis and Sundberg (Ref. 2) demonstrated the phenomenon adequately.

2.3 Oscillatory Problems

Modern sounding rockets are generally very long, slender; flexible structures. Even a system that has been very carefully designed to avoid such problems as aeroelastic divergence and roll-yaw resonance may still have serious oscillatory problems. This is a relatively new idea since it was first noted in 1963 and reported during the development of the Nitehawk 9 (Ref. 3). The typical motion of a rocket in an extra-atmospheric coning motion is discussed in detail in Chapter VI. Stone (Ref. 4 and 5) showed mathematically the possibility of a highly nonlinear magnus moment as the culprit in the extra-atmospheric coning motion. Reis and Sundberg (Ref. 2) showed that the same coning motion may be caused by bent motor structures.

Aeroelastic alteration of aerodynamic properties, lee-side vortices, warped fins and many more causes have been postulated as causes of some strange oscillatory motions. These problems are presently being investigated by many agencies and from several different viewpoints.

CHAPTER III

A LOOK AT THE PRESENT STATE-OF-THE-ART

The design approach for a sounding rocket system includes:

1. Ballistic analysis in which flight path, apogee, range and dispersion data are determined.
2. Static stability analysis where the relationship of the cg to the cp is determined.
3. Rigid-body dynamic stability analysis where aerodynamic pitching frequency and roll rate relationships are determined.
4. Aeroelastic divergence analysis where structural integrity is assured.

The oscillatory problems are generally being attacked in one of the following ways.

3.1 Structural Coupling Approach

There are several root locus methods for quantitatively determining the effects of changes in aeroelastic and aerodynamic characteristics on missile stability. Prince (Ref. 6) has a good example of this approach. It assumes that the aerodynamic and

aeroelastic characteristics of the system are well established and are well-behaved. The differential equations used in this type of study couple second-order equations for each elastic degree of freedom to the so-called "rigid-body" equations of motion. The elastic degrees of freedom are usually the normal modes of vibration of the structure. The stability of the system is determined by an analysis of the roots of the characteristic equations.

3.2 Influence Coefficient Matrix Approach

Some investigators use the influence coefficient method to solve the oscillatory type of problems. This is a highly specialized field that developed from the aircraft flutter field. The basic matrix equation is

$$q_i = \frac{\omega^2}{1 + ig} (K_{ij})(m_{ij}) + (A_{ij})\, q_i \qquad (1)$$

where:

1. (K_{ij}) is the structural influence coefficient and is generally an experimentally determined matrix.
2. q_i is the modal shape.
3. (A_{ij}) is the oscillatory aerodynamic influence coefficient matrix.
4. ω is the angular frequency of the assumed motion.
5. The inertia matrix of the structure is (m_{ij}).
6. The term (ig) accounts for the structural damping.

Abraham (Ref. 7) gave a clear explanation of this phenomenon.

3.3 Critical Load Approach

Several investigators have studied the stability of a flexible missile by idealizing the structure as a uniform beam under an end thrust. Assuming simple beam theory allows the use of the following equations:

$$\partial^2 u/\partial x^2 = (m/AE)\,(\partial^2 u/\partial t^2) \tag{2}$$

$$EI\left(\frac{\partial^4 y}{\partial x^4}\right) + \frac{\partial}{\partial x}\left[P\left(\frac{\partial y}{\partial x}\right)\right] + m\frac{\partial^2 y}{\partial t^2} - p = 0 \tag{3}$$

where m is mass per unit length, y is the lateral coordinate, u is the deflection, A the cross sectional area, EI the bending stiffness, P(x, t) the longtitudinal force, and p(x, t) represents the lateral load other than inertia loading. Proper boundary conditions are established and generally , nonuniform mass and stiffness, structural damping, transient response, aerodynamic forces, and shear and rotary inertia are all neglected. A suitable approximation method, e.g., like the Galerkin procedure, is used to change the equation into a set of ordinary differential equations. Specific cases are then studied on the computer to determine the critical load for the beam. Beal (Ref. 8) gave a good example of this type of analysis.

CHAPTER IV

DEVELOPMENT OF THE METHOD

4.1 Discussion of Analytical Philosophy

Nearly all investigations of the dynamic characteristics of elastic vehicles can be neatly categorized into three distinct groups:

1. The theoretical approach where a great deal of rigorous mathematics leads to conclusions only for simplified cases. This type of investigation breaks new ground, asks new questions and certainly challenges the technology to move forward. However, this type may not be applicable to the present problems or the mathematics involved may be so difficult that, in a practical sense, only simple examples can be solved. Meirovitch and Wesley (Ref. 9) presented an outstanding mathematical analysis which was used to solve only two simplified flight problems. Stone (Ref. 4) challenges the rocket engineers to include magnus moments in their analyses. However, at this stage of rocket development, no one has measured quantitatively how much an actual magnus moment alters the flight characteristics of

any of the present rocket systems.

2. The similitude approach which uses scale models and wind tunnels to determine static and dynamic characteristics of the model being tested. The model is tested to the full range of the tunnel and then scaling factors are used to convert these data into meaningful parameters for an actual flight system. The fact that this type of analysis has become very sophisticated is clearly shown in the report by Hanson and Doggett (Ref. 10).

3. The flight data approach where the analyst uses flight data to calculate the effective values of parameters entering into the aerodynamic equations. The effective values are compared to theoretical values and the effect of elasticity of the body is estimated. This method has not been developed to a high degree of sophistication but Reis and Sundberg (Ref. 2) advanced the method somewhat.

There are some obvious and some not so obvious disadvantages to each of these approaches. However, all share a common disadvantage; i.e., each formulates the problem in the mathematical and manipulation manner most suited to a particular type of analysis. This causes the field to advance in three different areas but it also leads to a breakdown in communications between the fields. Furthermore, it leaves the development engineer without the necessary

tools to advance the development of actual flight system.

The purpose of this dissertation is to develop a fourth approach that might be called the integrated approach. The scheme would be to develop a set of differential equations that describe the motion of the elastic vehicle in such a manner that almost any part of the motion can be determined separately and combined along with other motions into the equations. There are probably several forms that would allow such a combination but the equations derived in Appendix A and used in this dissertation are similar in form to the equations derived by Young (Ref. 11) for the planar case. The advantages of this system are:

1. It allows the use of equations of motion that have good theoretical foundations and use a minimum of simplifying assumptions.
2. The inputs into the equations can be determined from established procedures.
3. New information can be included easily.
4. The equations are in a form that is generally recognized. For example, the angular motion equations are the Euler equations and the elastic coupling is included in the applied moments.

4.2 The Basic Assumptions

In the formulation of the problem, simplifying assumptions must be held to a minimum. However, it generally is necessary to make some assumptions which not only simplify but serve to define the problem. In this dissertation the following assumptions are made:

1. The mass is a function of x only.
2. The lateral bending is governed by linear theory of Timoshenko beams.
3. The torsional rigidity is assumed to be infinite.
4. The deflections of the beam relative to the moving axes are represented by normal mode oscillations.
5. Structural damping is neglected.

4.3 The Coordinate System

Figure 1 shows the general coordinate system. The velocity of the center of mass is denoted by V_o and it is directed along the tangent to the trajectory of the center of mass. The missile configuration is described relative to a set of moving axes (x, y, and z) which has its origin fixed at the center of mass. It is a righthanded orthogonal system that is fixed in the missile body and coincides with the undeflected missile principal axes. The x-axis is directed along the longitudinal axis of symmetry of the undeflected missile. Longitudinal deformations along the x axis are denoted by u_1, along the y axis by u_2 and along the z axis by u_3.

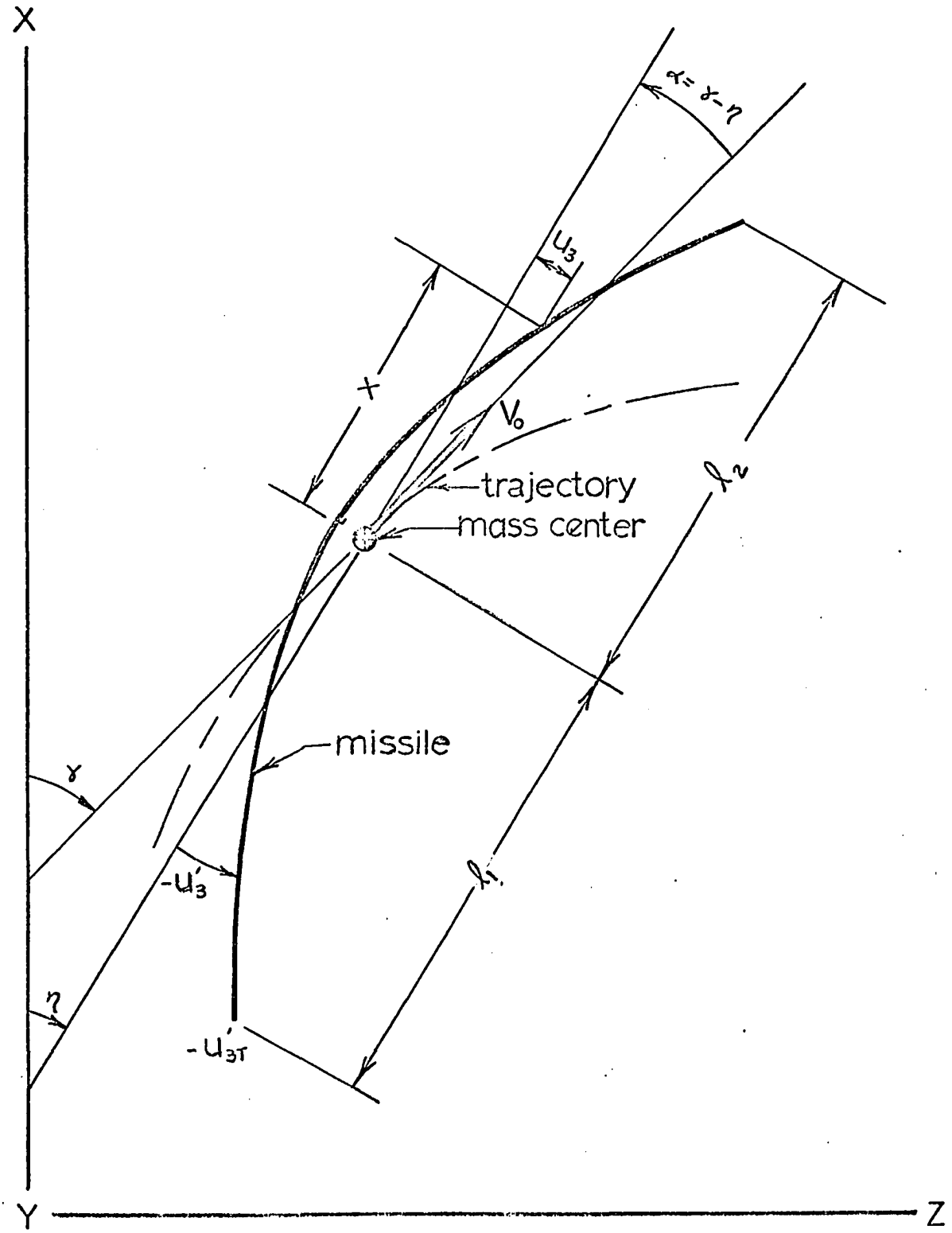

Figure 1 The Coordinate System

The inclination of the x axis from the vertical is denoted by η and the inclination of the trajectory tangent is γ. Rotation about the x axis is denoted by θ_1 (roll), about the y axis by θ_2 (pitch) and about the z axis by θ_3 (yaw). The coordinate system is oriented so that the x axis is in the trajectory plane.

4.4 The Differential Equations of Motion

The differential equations are shown in this section with a brief explanation for each set of equations. A complete derivation is shown in Appendix A. The displacement equations are written as follows:

$$\left.\begin{aligned} u_1(x,t) &= \sum_{i=1}^{\infty} \phi_i \cdot q_i(t) \\ u_2(x,t) &= \sum_{j=1}^{\infty} T_j \cdot q_j(t) \\ u_3(x,t) &= \sum_{k=1}^{\infty} \sigma_k \cdot q_k(t) \end{aligned}\right\} \quad (4)$$

where ϕ_i, T_j, σ_k are the eigenfunctions of a free-free beam and q_i, q_j and q_k are the corresponding generalized coordinates. Now considering the corresponding angles of rotation of a missile element, the element rotation equations are

$$\left.\begin{aligned} \Psi(x,t) &= \sum_{k=1}^{\infty} \psi_k \cdot q_k(t) \\ \Lambda(x,t) &= \sum_{j=1}^{\infty} \lambda_j(x) \cdot q_j(t) \end{aligned}\right\} \quad (5)$$

There is no equation for an element rotating about the x axis because of the assumption that the missile is rigid in that plane. The accelerations of the center of mass can be written by referring to Figure 1. It should be noted that the total angular rotation of a point on the missile axis is not simply θ_2 about the y axis and θ_3 about the z axis. Making a small angle assumption, the rotation in the pitch plane (xz plane) is $\theta_2 + \partial u_3/\partial x$ and the rotation in the yaw plane (xy plane) is $\theta_3 + \partial u_2/\partial x$. Therefore, the total pitch angle is not $\alpha = \gamma - \theta_2$ but $\alpha_T = \gamma - \theta_2 - \partial u_3/\partial x$. The total yaw angle of attack is $\beta = \theta_3 + \partial u_2/\partial x$. With this in mind, the acceleration components of the center of mass can now be written in terms of the flight-path velocity and coordinates as:

$$\begin{aligned} \bar{A}_x &= \dot{V}_o \cos\alpha - V_o \dot{\gamma} \sin\alpha \\ \bar{A}_y &= \dot{V}_o \cos\beta - V_o \dot{\beta} \sin\beta \\ \bar{A}_z &= \dot{V}_o \sin\alpha + V_o \dot{\gamma} \cos\alpha \end{aligned} \tag{6}$$

Using Newton's second law and referring to Figure 2, the equations of motion for the center of mass are:

$$\begin{aligned} M(x)\bar{A}_x &= T^* - Mg\cos\eta + F_x^* \\ M(x)\bar{A}_y &= T^* u'_{3T} + F_y^* - J_{Dy} \\ M(x)\bar{A}_z &= T^* u'_{3T} + Mg\sin\eta - J_{Dz} + F_z^* \end{aligned} \tag{7}$$

The accelerations are determined from Figure 3; also see Appendix A. In the derivation of these equations, T^* is the motor thrust and the angle of inclination from the vertical, η, is assumed to be

$P_z(x,t)$ - Normal Force in XZ Plane

$P_y(x,t)$ - Normal Force in XY Plane

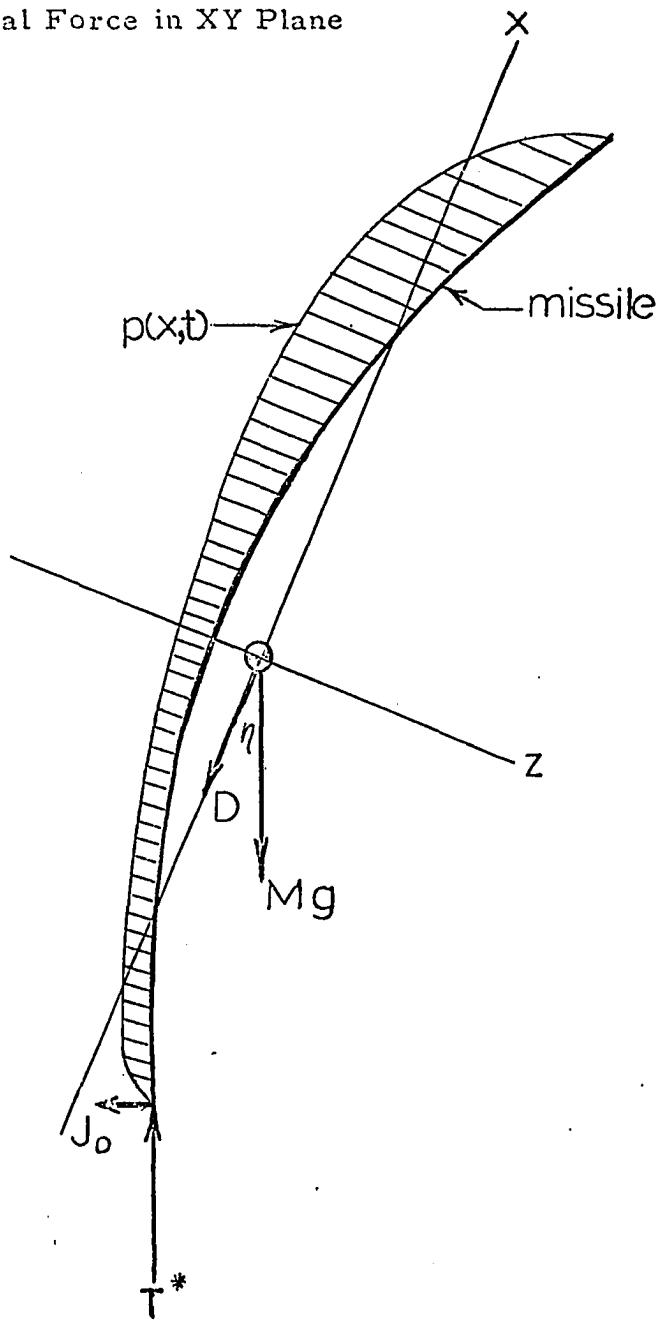

Figure 2 The Force System

Axis	Displ.	Unit Vector	Rotation
x	u_1	$\bar{i}$	θ_1
y	u_2	$\bar{j}$	θ_2
z	u_3	$\bar{k}$	θ_3

$\bar{P}$ - Position vector from inertial axis to arbitrary point

$\bar{R}$ - Position vector to center of mass.

$\vec{\rho}$ - Position vector in moving coordinates

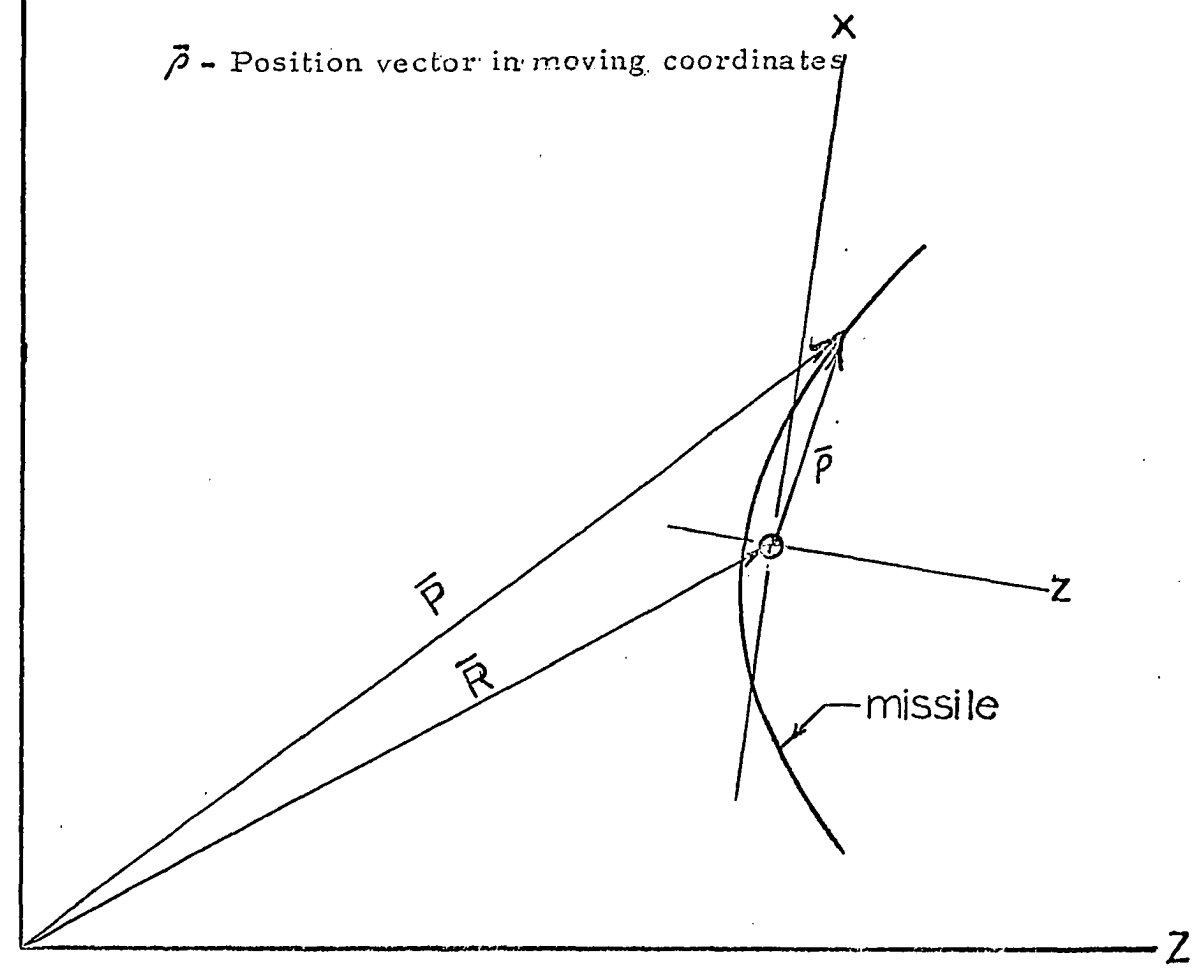

Figure 3 The Kinematic System

small. Therefore, T^* in the x equation is assumed to be directed along the x axis, u'_{2T} is the slope of the displacement in the y direction at the tail of the missile and is, therefore, approximately equal to the angle of deflection, and u'_{3T} is the tail slope in the z direction. The resultant aerodynamic forces in the x, y, and z directions are F_x^*, F_y^* and F_z^*. Here F_x^* is approximately equal to the drag; F_y^* and F_z^* are approximately equal to the normal force in the xy and xz planes; J_{Dy} and J_{Dz} are the jet damping terms in the xy and xz planes. The normal forces are actually distributed forces and may be estimated by several methods.

The equations of rotation were derived using Lagrange's equation and the assumption that the instantaneous mass moment of inertia can be approximated by the rigid-body mass moment of inertia. The equations of rotation are:

$$
\begin{aligned}
I_{xx}\ddot{\theta}_1 &= M_{\theta 1}^* \\
I_{yy}\ddot{\theta}_2 + (I_{xx} - I_{zz})\dot{\theta}_1\dot{\theta}_3 &= (J_{D_z} - T^* u'_{3T})_1 + T^* u_{3T} + M^*_{\theta 2} \\
I_{zz}\ddot{\theta}_3 + (I_{yy} - I_{xx})\dot{\theta}_1\dot{\theta}_2 &= (J_{D_y} - T^* u'_{2T})_1 + T^* u_{2T} + M^*_{\theta 3}
\end{aligned}
\tag{8}
$$

where $M^*_{\theta_r}$ is the moment about the center of mass during the angular displacement $\Delta\theta_r$ $(r = 1, 2, 3)$.

The bending equations were also derived using a form of Lagrange's equation. These equations are:

For the xz plane:

$$M(\ddot{q}_k + \omega_k^2 q_k) = \int_{-\ell_1}^{\ell_2} P_{xz}(x,t)\sigma_k(x)dx + T^* u_3'(-\ell_1) \tag{9}$$

For the xy plane:

$$M(\ddot{q}_j + \omega_j^2 q_j) = \int_{-\ell_1}^{\ell_2} P_{xy}(x,t)T_j'(x)dx + T^* u_2' T_j(-\ell_1)$$

where ω_i is the circular frequency of the ith mode.

CHAPTER V

APPLICATION OF THE INTEGRATED METHOD

5.1 Introduction

The purpose of the example is to demonstrate the use of the equations and to compare the motions obtained from the solution of the equations with actual flight data. This example will determine the motion of a typical second stage of the Nitehawk 9 during the period from motor burnout to exit from the atmosphere. The typical second stage and a typical trajectory are described in "The Nitehawk 9" (Ref. 3).

The equations derived in Appendix A are expressed in a body-fixed coordinate system. This was done to simplify the separation of the equations into four major parts: the motion of the center of mass, the rigid body rotational motion, the structural deflections and the vibrational motion of the elastic system. It also allowed the equations to be expressed in terms more familiar to structural engineers. However, this approach puts the equations in an inconvenient form that is difficult to use. To solve this example, the equations will be transformed to the "aeroballistic system".

The so-called aeroballistic reference system is a system of axes with its origin fixed at the center of mass of the rocket and that pitchs and yaws with the body but does not roll with the body (see Figure 4). The equations of motion are transformed from the body-fixed system to the aeroballistic system in Appendix B. After the transformation, the displacement equations, mass-center translational equations, and bending equations are unchanged from Equations (4), (7) and (9), respectively. However, the equations of rotation, Equations (8), become

$$
\begin{aligned}
I_{xx}\,\ddot{r}_1 &= M^*_{r_1} \\
I_{yy}\,\ddot{r}_2 + I_{xx}\,\dot{r}_1\,\dot{r}_3 &= (J_{Dz} - T^* u'_{3T})\ell_1 + T^* u_{3T} + M^*_{r_2} \\
I_{zz}\,\ddot{r}_3 - I_{xx}\,\dot{r}_2\,\dot{r}_3 &= (J_{Dy} - T^* u'_{2T})\ell_1 + T^* u_{2T} + M^*_{r_3}
\end{aligned}
\tag{10}
$$

where r_1, r_2, r_3 are the roll, pitch and yaw angles respectively.

5.2 General Approach

The general approach to this problem is to use the tools that are normally available to the sounding rocket designer to solve for the inputs to an analog computer; the analog computer will take the flight and structural inputs and determine the oscillatory motion of the rocket system. The output of the computer will then be compared to actual flight data from Nitehawk 9 flights. The analog

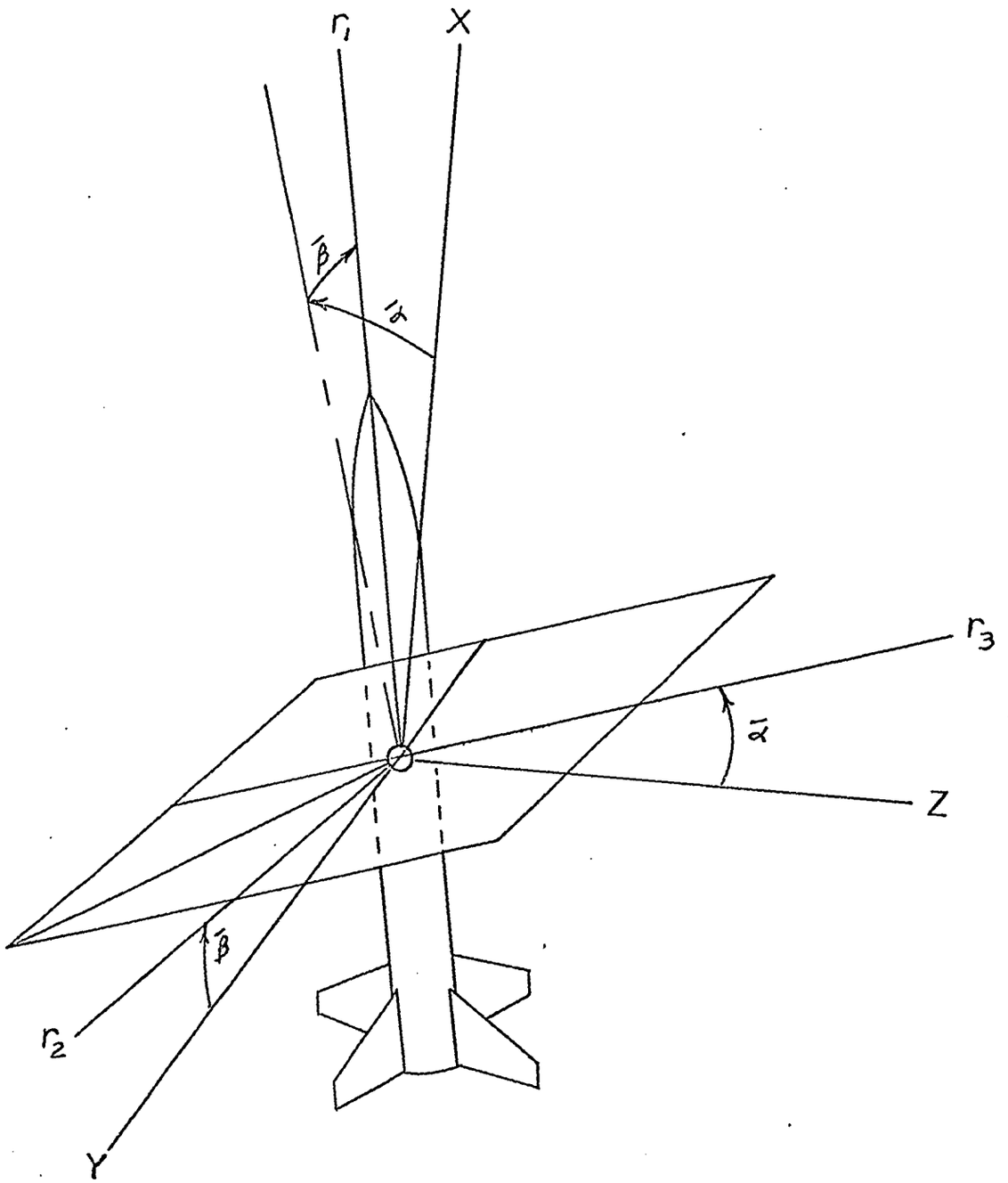

Figure 4 The Aeroballistic Reference System

computer is described in Appendix E.

5.3 System Description

The overall dimensions of the second stage of a Nitehawk 9 are shown in Figure 6. The weight and EI distribution are shown in Figures 7 and 8. The vehicle is 207 inches long and weighs 255 pounds at burnout. The payload is 68 inches long and weighs 125 pounds. The vehicle has a pitch (and yaw) moment of inertia of 335.0 slug/ft^2 and a roll moment of inertia of 1.96 slug/ft^2. The vehicle center of mass is at station 105.6 inches. The chart below shows the thrust vs. time curve for the Tomahawk motor which propels the Nitehawk 9.

Figure 5 From (Ref. 3)

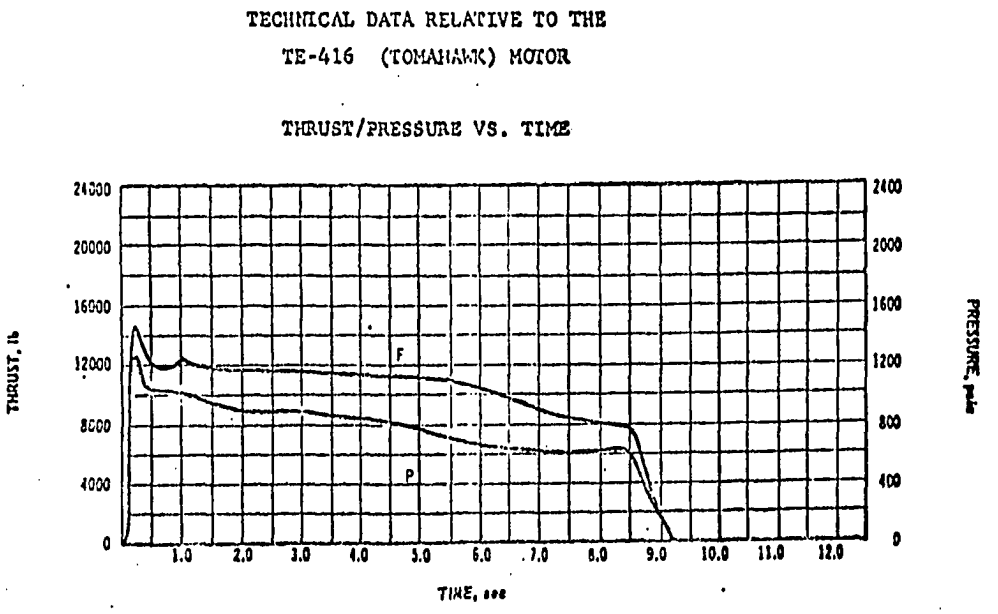

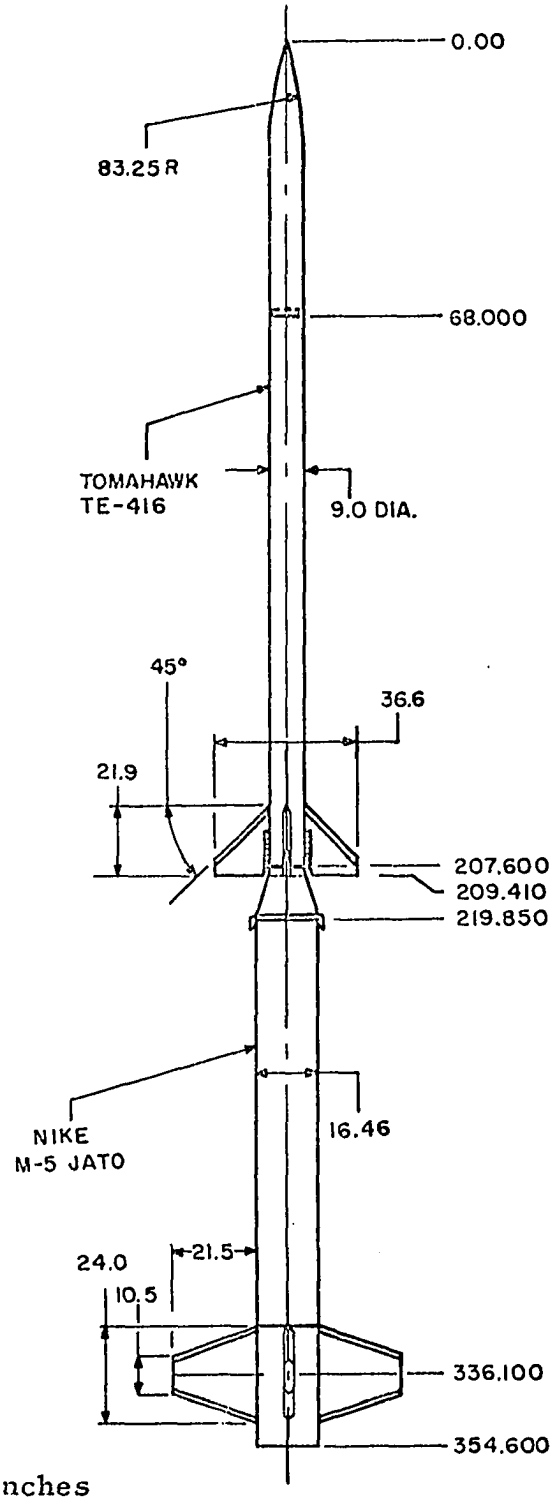

All Dimensions in inches

Figure 6 The Nitehawk 9 from (Ref. 3)

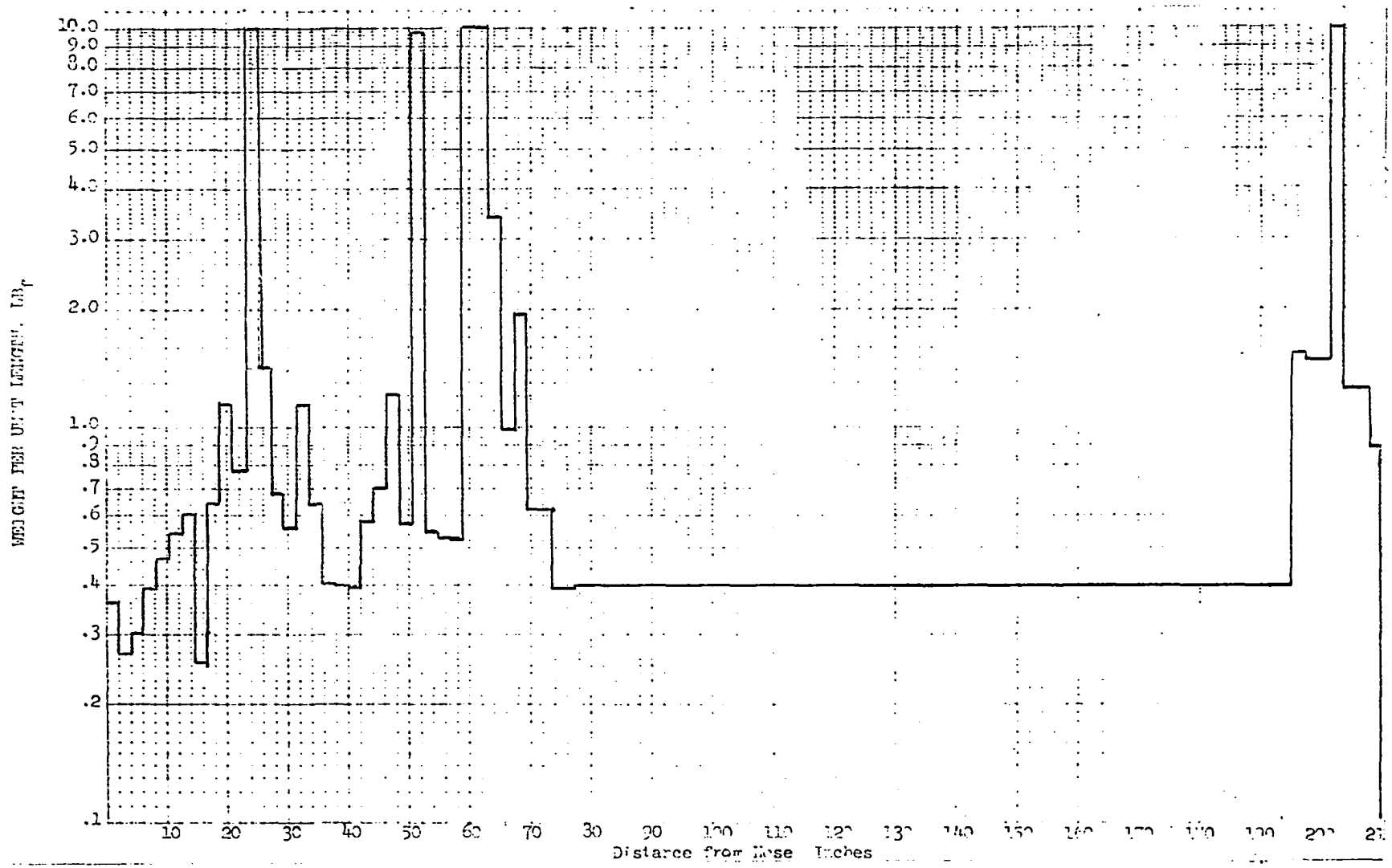

Figure 7 Weight Distribution for Tomahawk Motor and 9 inch Payload
(From Ref. 18)

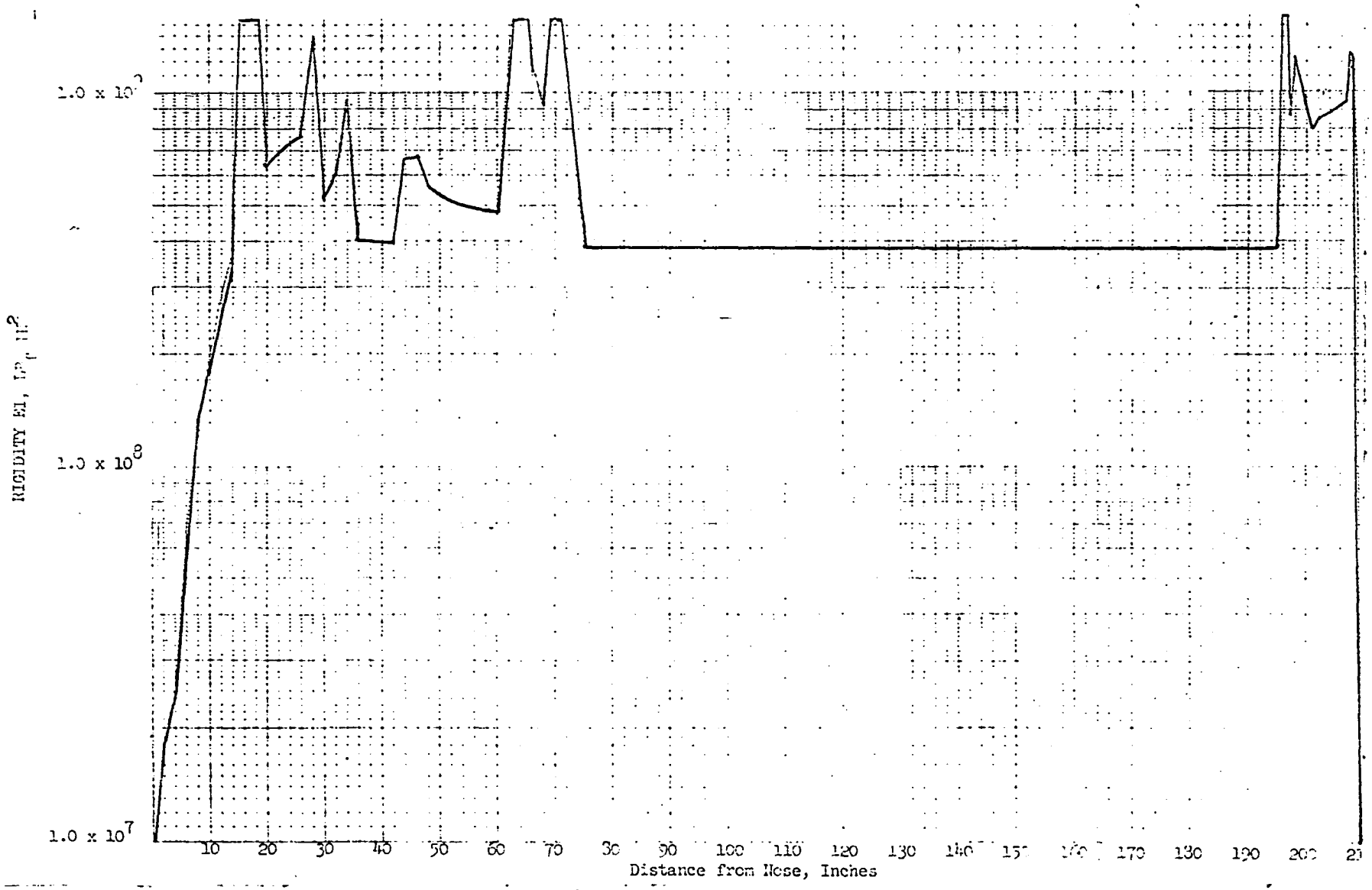

Figure 8 EI Distribution for Tomahawk Motor and 9 inch Payload (From Ref. 18)

5.4 Formulation of the Problem

The motion of the center of mass of the vehicle is simply a point-mass trajectory as shown in Table 1. Table 1 is a point-mass trajectory of the second stage of a Nitehawk 9 and was extracted from the development report of that system (Ref. 3). From this trajectory, the general path of the body and some aerodynamic forces may be obtained.

The deflection of the body and the vibrational motions result in moments that are applied to the moment equations. These two moments and all other moments are determined in Appendix C.

In order to get the equations on the analog machine, it was necessary to combine some terms in the rotational equations, Equations (10). This changes the looks of the equations but they are, in fact, the same equations. The equations are rewritten as follows:

$$
\begin{aligned}
I_{xx}\ddot{r}_1 &= M^*_{r_1} \\
I_{yy}\ddot{r}_2 + \dot{r}_1 \dot{r}_3 I_{xx} &= M^*_{r_2} \\
I_{zz}\ddot{r}_3 - \dot{r}_2 \dot{r}_1 I_{xx} &= M^*_{r_3}
\end{aligned}
\tag{11}
$$

where

$$
\begin{aligned}
M^*_{\dot{r}_2} &= f_1(t)\, r_2(57.3) - f_2(t)\dot{r}_2 + f_4(t)\, r_2(0) \\
M^*_{r_3} &= f_1(t)\, r_3(57.3) - f_2(t)\dot{r}_3 + f_5(t)\, r_3(0)
\end{aligned}
\tag{12}
$$

Table 1 (from Ref. 3)

Typical Nitehawk 9 Trajectory; Second-Stage Ignition 12 Seconds

Run 6

INPUT DATA

THETA	PSI	ALT	VEL	RANGE	W0	W1	W2	W3	T0	T1	T2	T3	T4	T5
80.00	0.	0.	2.0	0.	1984.0	1251.0	664.0	267.0	0.	0.	3.54	0.	12.00	20.95

THR 1	THR 2	DRAG 1	DRAG 2	DRAG 3	DRAG 4	S1	S2	L	C1	C2	DRT	AT	1	5	6
1.0300	1.0500	1.0000	1.0000	1.0000	1.000	1.4741	0.4418	16.0	0.65	0.65	0	3	1	0	1

THR 1C	THR 1C	WINCN	INST	GZERO
82	181	0	9000.0	32.174

TIME	THETA	PSI	ALT	VEL	RANGE	EAST	NORTH	MACH	ACC	THR	DR	Q
0.	80.00	0.	0.	2.0	0.	0.	0.	0.00	-0.	0.	-0.	0.00
0.22	80.00	0.	14.6	141.4	2.6	0.	2.6	0.13	687.1	720.0	-0.2	23.75
0.50	79.60	0.	80.4	337.6	14.5	0.	14.5	0.30	714.9	747.8	-1.2	146.91
1.00	79.26	0.	336.3	708.0	62.4	0.	62.4	0.63	767.1	804.7	-5.9	615.95
1.50	79.07	0.	780.2	1103.3	147.5	0.	147.5	0.99	805.9	877.6	-40.1	1455.82
2.00	78.93	0.	1422.7	1520.6	272.5	0.	272.5	1.37	869.0	972.9	-72.3	2695.59
2.50	78.83	0.	2278.8	1975.6	440.8	0.	440.8	1.78	941.5	1083.3	-110.2	4418.14
3.00	78.75	0.	3359.6	2417.2	655.1	0.	655.1	2.19	767.5	950.7	-151.6	6361.62
3.38	78.69	0.	4301.0	2584.3	842.9	0.	842.9	2.35	20.4	182.1	-167.4	6979.04
3.50	78.68	0.	4604.4	2569.5	903.6	0.	903.6	2.34	-147.4	0.	-115.8	6820.49
4.00	78.60	0.	5846.3	2498.1	1153.1	0.	1153.1	2.28	-138.7	0.	-107.1	6209.09
4.50	78.53	0.	7053.9	2430.8	1397.3	0.	1397.3	2.23	-130.7	0.	-99.2	5666.02
5.00	78.45	0.	8229.1	2367.3	1636.6	0.	1636.6	2.18	-123.5	0.	-92.0	5182.01
5.50	78.37	0.	9373.8	2307.2	1871.2	0.	1871.2	2.14	-116.9	0.	-85.4	4750.68
6.00	78.20	0.	10489.5	2250.3	2101.6	0.	2101.6	2.09	-110.9	0.	-79.4	4365.11
6.50	78.21	0.	11577.7	2196.2	2327.9	0.	2327.9	2.05	-105.4	0.	-73.9	4018.16
7.00	78.12	0.	12639.8	2144.8	2550.5	0.	2550.5	2.01	-100.3	0.	-68.9	3705.25
7.50	78.03	0.	13677.0	2095.8	2769.5	0.	2769.5	1.97	-96.0	0.	-64.5	3420.89
8.00	77.94	0.	14690.3	2048.8	2985.1	0.	2985.1	1.94	-92.1	0.	-60.6	3144.38
8.50	77.84	0.	15680.8	2003.7	3197.6	0.	3197.6	1.90	-88.4	0.	-57.0	2911.10
9.00	77.75	0.	16649.3	1960.4	3407.1	0.	3407.1	1.87	-85.0	0.	-53.6	2699.98
9.50	77.64	0.	17596.7	1918.7	3613.8	0.	3613.8	1.83	-81.8	0.	-50.4	2506.12
10.00	77.54	0.	18523.8	1878.5	3817.7	0.	3817.7	1.80	-78.8	0.	-47.5	2329.84
10.50	77.43	0.	19431.3	1839.8	4019.1	0.	4019.1	1.77	-76.1	0.	-44.7	2180.39
11.00	77.32	0.	20319.8	1802.4	4218.1	0.	4218.1	1.74	-73.5	0.	-42.1	2030.85
11.50	77.21	0.	21190.0	1766.3	4414.7	0.	4414.7	1.71	-71.1	0.	-39.7	1894.10
12.00	77.09	0.	22042.4	1731.3	4609.2	0.	4609.2	1.68	-68.7	0.1	-37.5	1771.63
12.50	76.98	0.	22938.1	1931.9	4815.4	0.	4815.4	1.89	584.8	651.7	-35.6	2162.70
13.00	76.88	0.	23952.4	2237.3	5050.9	0.	5050.9	2.19	636.9	711.7	-43.6	2794.92
13.50	76.79	0.	25118.6	2552.5	5323.8	0.	5323.8	2.51	624.2	707.6	-52.1	3487.64
14.00	76.71	0.	26437.2	2867.1	5634.2	0.	5634.2	2.84	634.7	725.4	-59.5	4194.43
14.50	76.64	0.	27910.8	3193.3	5983.2	0.	5983.2	3.18	669.9	768.6	-67.5	4930.49
15.00	76.58	0.	29547.1	3538.3	6372.7	0.	6372.7	3.55	710.9	819.1	-76.9	5703.50
15.50	76.52	0.	31355.4	3901.5	6805.1	0.	6805.1	3.95	742.9	859.9	-85.8	6499.12
16.00	76.47	0.	33343.9	4281.5	7282.7	0.	7282.7	4.37	777.4	905.3	-96.8	7261.29
16.50	76.42	0.	35521.2	4680.9	7807.6	0.	7807.6	4.82	821.7	960.1	-107.2	7940.42
17.00	76.38	0.	37897.4	5100.8	8382.5	0.	8382.5	5.27	850.6	998.7	-117.0	8483.07
17.50	76.34	0.	40479.1	5525.7	9009.2	0.	9009.2	5.71	849.2	1004.6	-124.3	8795.36
18.00	76.30	0.	43263.9	5933.2	9687.1	0.	9687.1	6.13	780.3	940.3	-128.8	8893.32
18.50	76.26	0.	46241.8	6330.8	10414.1	0.	10414.1	6.54	810.3	971.3	-129.9	8766.34
19.00	76.23	0.	49416.1	6714.3	11191.1	0.	11191.1	6.97	845.3	1005.9	-129.4	8520.78
19.50	76.20	0.	52794.2	7170.2	12020.0	0.	12020.0	7.41	858.5	1017.5	-127.9	8226.34
20.00	76.17	0.	56380.5	7603.8	12901.9	0.	12901.9	7.85	875.6	1030.5	-123.8	7783.47
20.50	76.14	0.	60177.8	8029.1	13837.9	0.	13837.9	8.29	720.9	869.0	-117.1	7206.05
20.94	76.12	0.	63655.7	8201.6	14696.7	0.	14696.7	8.47	-17.6	96.8	-101.3	6387.03
21.00	76.11	0.	64133.4	8195.1	14814.8	0.	14814.8	8.47	-142.5	0.	-111.5	6192.37
21.50	76.09	0.	68094.5	8129.0	15795.0	0.	15795.0	8.40	-122.6	0.	-91.6	5055.95
22.00	76.06	0.	72025.3	8072.0	16769.8	0.	16769.8	8.34	-107.0	0.	-76.0	4178.09
22.50	76.03	0.	75929.6	8021.7	17740.0	0.	17740.0	8.29	-94.3	0.	-63.3	3459.88
23.00	76.00	0.	79810.7	7977.6	18706.3	0.	18706.3	8.24	-81.9	0.	-50.9	2766.83
23.50	75.98	0.	83671.2	7938.8	19669.6	0.	19669.6	8.18	-73.8	0.	-42.9	2320.95
24.00	75.95	0.	87513.3	7903.8	20630.2	0.	20680.2	8.08	-66.2	0.	-35.3	1889.19
24.50	75.92	0.	91338.9	7872.5	21588.7	0.	21588.7	7.98	-59.7	0.	-28.8	1532.11
25.00	75.89	0.	95149.5	7843.7	22545.4	0.	22545.4	7.89	-55.2	0.	-24.3	1262.16
25.50	75.86	0.	98946.3	7817.2	23500.7	0.	25500.7	7.81	-50.7	0.	-19.8	1017.35
26.00	75.83	0.	102730.3	7792.7	24454.8	0.	24454.8	7.73	-47.6	0.	-16.7	857.18
26.50	75.81	0.	106502.3	7769.6	25407.8	0.	25407.8	7.65	-44.9	0.	-14.1	719.63
27.00	75.78	0.	110262.9	7747.8	26360.0	0.	26360.0	7.57	-42.4	0.	-11.5	584.55
27.50	75.75	0.	114012.8	7727.0	27311.5	0.	27311.5	7.50	-40.8	0.	-9.9	499.68
28.00	75.72	0.	117752.2	7707.0	28262.4	0.	28262.4	7.43	-39.2	0.	-8.3	416.00
28.50	75.69	0.	121481.7	7687.8	29212.7	0.	29212.7	7.36	-37.8	0.	-7.0	349.39
29.00	75.66	0.	125201.6	7669.2	30162.6	0.	30162.6	7.30	-36.8	0.	-6.0	298.41
29.50	75.63	0.	128912.0	7651.0	31112.1	0.	31112.1	7.23	-35.8	0.	-5.1	248.07
30.00	75.60	0.	132613.3	7633.3	32061.4	0.	32061.4	7.17	-35.1	0.	-4.3	213.32
35.00	75.30	0.	169150.2	7468.6	41543.6	0.	41543.6	6.75	-31.8	0.	-1.0	44.19
40.00	74.98	0.	204866.5	7312.9	51018.1	0.	51018.1	7.14	-30.8	0.	-0.3	12.25
45.00	74.66	0.	239786.2	7160.1	60490.6	0.	60490.6	7.78	-30.4	0.	-0.1	3.00
50.00	74.32	0.	273917.7	7008.7	69962.6	0.	69962.6	8.28	-30.2	0.	-0.0	0.46
55.00	73.97	0.	307266.2	6858.1	79434.5	0.	79434.5	8.10	-30.0	0.	-0.0	0.08
60.00	73.60	0.	339831.5	6708.3	88906.3	0.	88906.3	7.92	-29.9	0.	-0.0	0.02

$$f_1(t) = T^*(u_{iT} - u'_{iT}\ell_1) - Mr_2 \qquad i = 2, 3$$

$$f_2(t) = M_{jD_k} + M_{q_k} \qquad k = y, z$$

$$f_4(t) = 0.0015 + 0.005 \sin \omega t \qquad \omega = 188 \text{ rad/sec.}$$
$$\text{or } 27 \text{ Hz}$$

$$f_5(t) = 0.0015 + 0.005 \cos \omega t$$

$$I_{xx} = 1.96 \text{ slug/ft}^2 \qquad (12) \text{ (Cont.)}$$

$$I_{yy} = 335 \text{ slug/ft}^2$$

Initial Conditions:

$$r_1(0) = 0$$

$$r_2(0) = 0 \qquad \dot{r}_2 = 0.882 \text{ rad/sec.}$$

$$r_3(0) = 0.035 \text{ rad} \qquad \dot{r}_3 = 0$$

The roll rate vs. time, $f_1(t)$ and $f_2(t)$ are shown in Figures 9, 10 and 11 respectively.

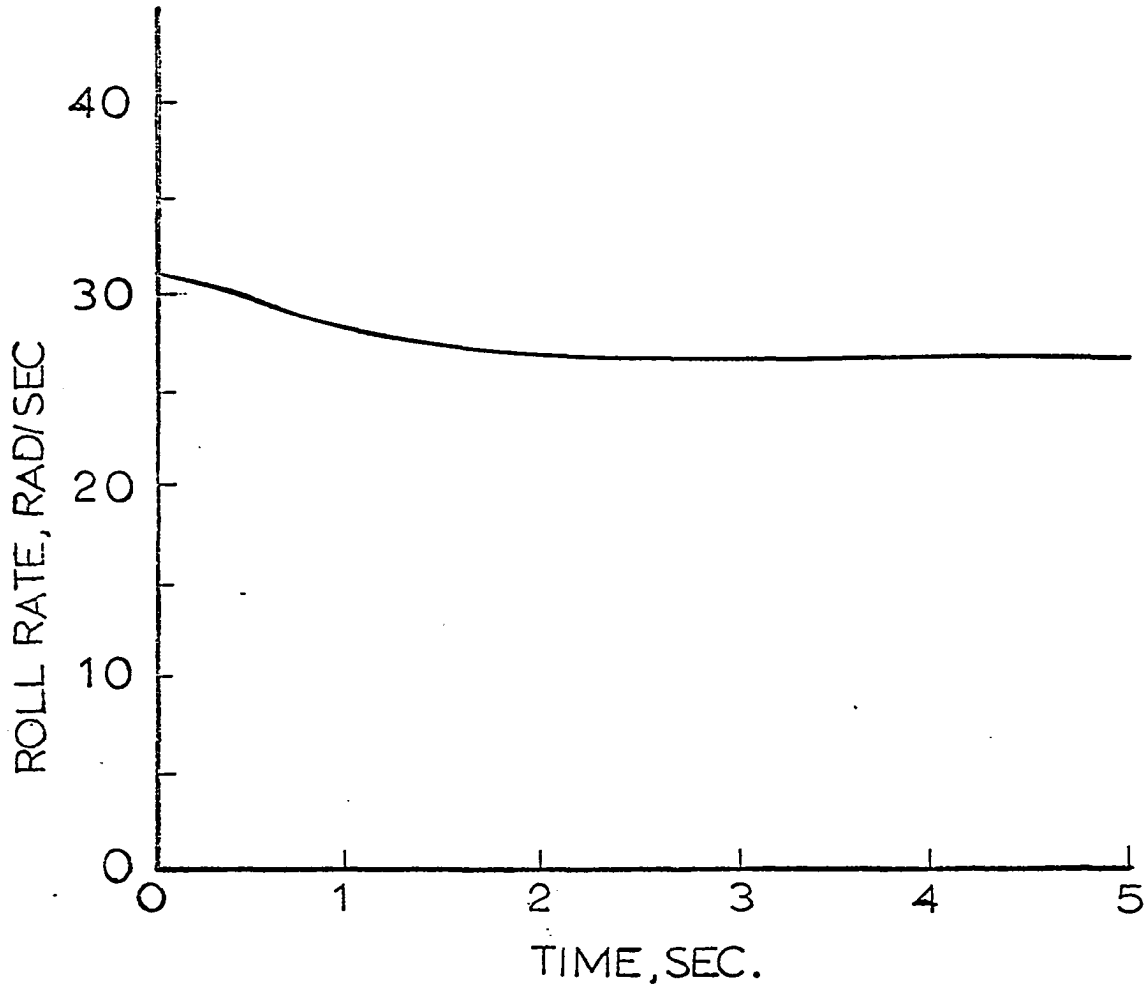

Figure 9 The Roll Rate vs. Time

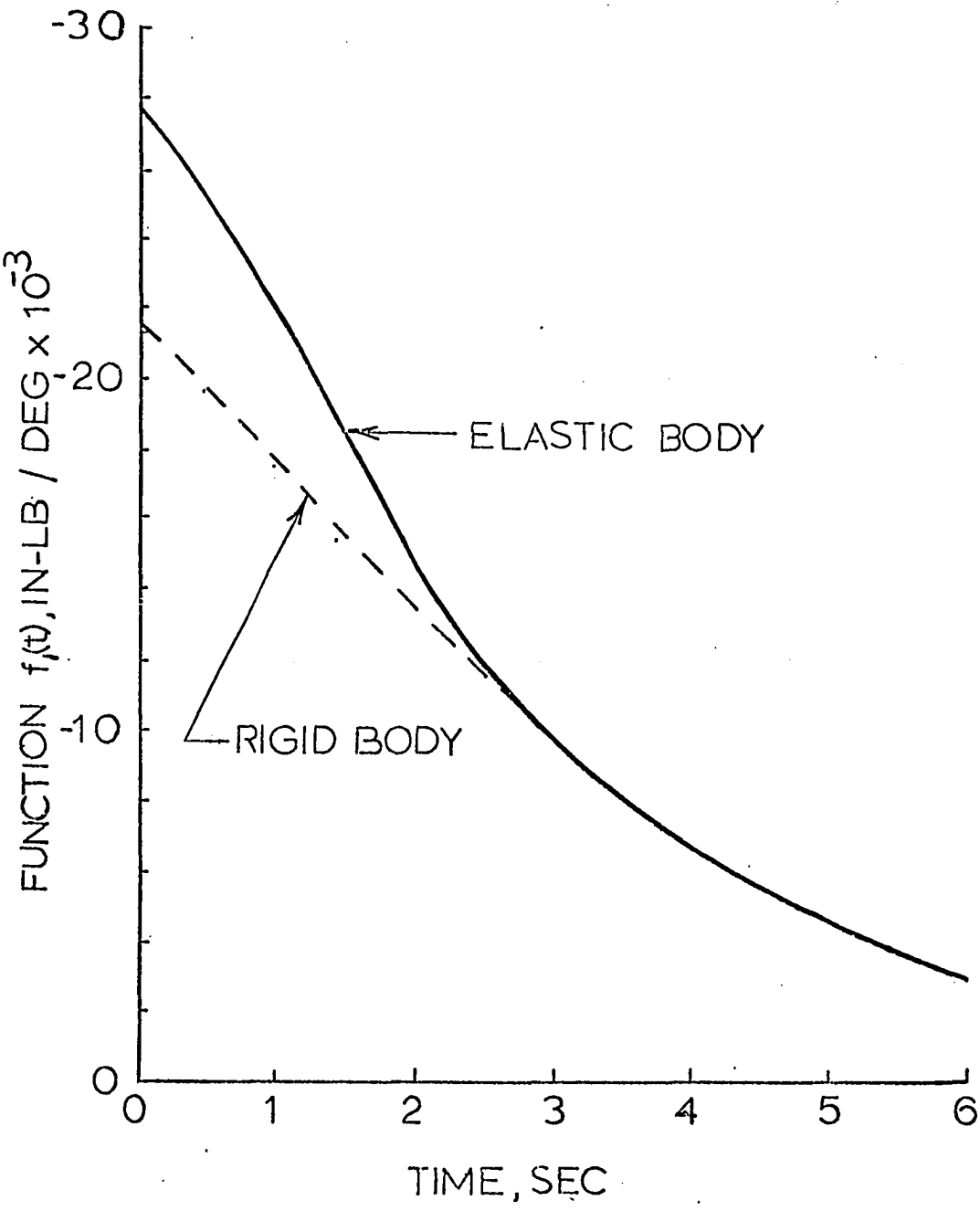

Figure 10 Function $f_1(t)$ vs. Time

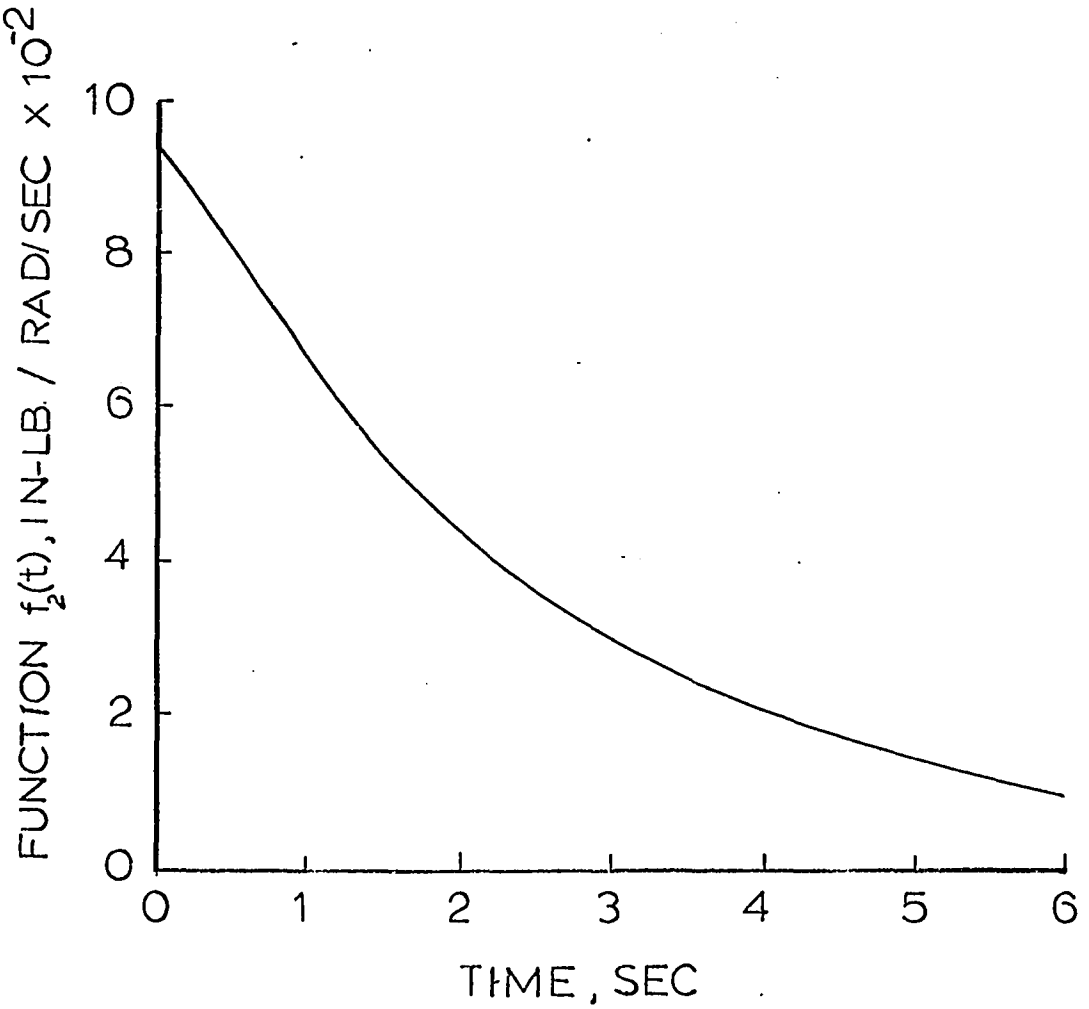

Figure 11 Function $f_2(t)$ vs. Time

CHAPTER VI

DISCUSSION OF RESULTS

The yaw gyro traces from actual Nitehawk 9 flights showing normal, locked-in (or roll-pitch coupled), and coning motion are shown in Figure 13 (from Ref. 13). In attempting to duplicate the motions shown, the approach was to use the same relatively standard restoring moments (function f_1) and aerodynamic damping (function f_2) moments as used for the normal flight. The other conditions are then added to duplicate the locked-in and coning flights.

Figure 13a shows the computer simulation of the normal or desired flight. It can be seen that the computer flight data simulate the actual flight data quite well. The vehicle has slight oscillatory motion at burnout; it damp slights and then diverges slightly as the vehicle leaves the atmosphere. This is shown to be a normal flight by Stone (Ref. 14).

Figure 13b shows a simulation of roll-pitch coupling. Notice that the motion is highly divergent when the roll rate is the same as the pitch frequency. The bent payload moment was used as the disturbing moment to cause the two frequencies to lock together.

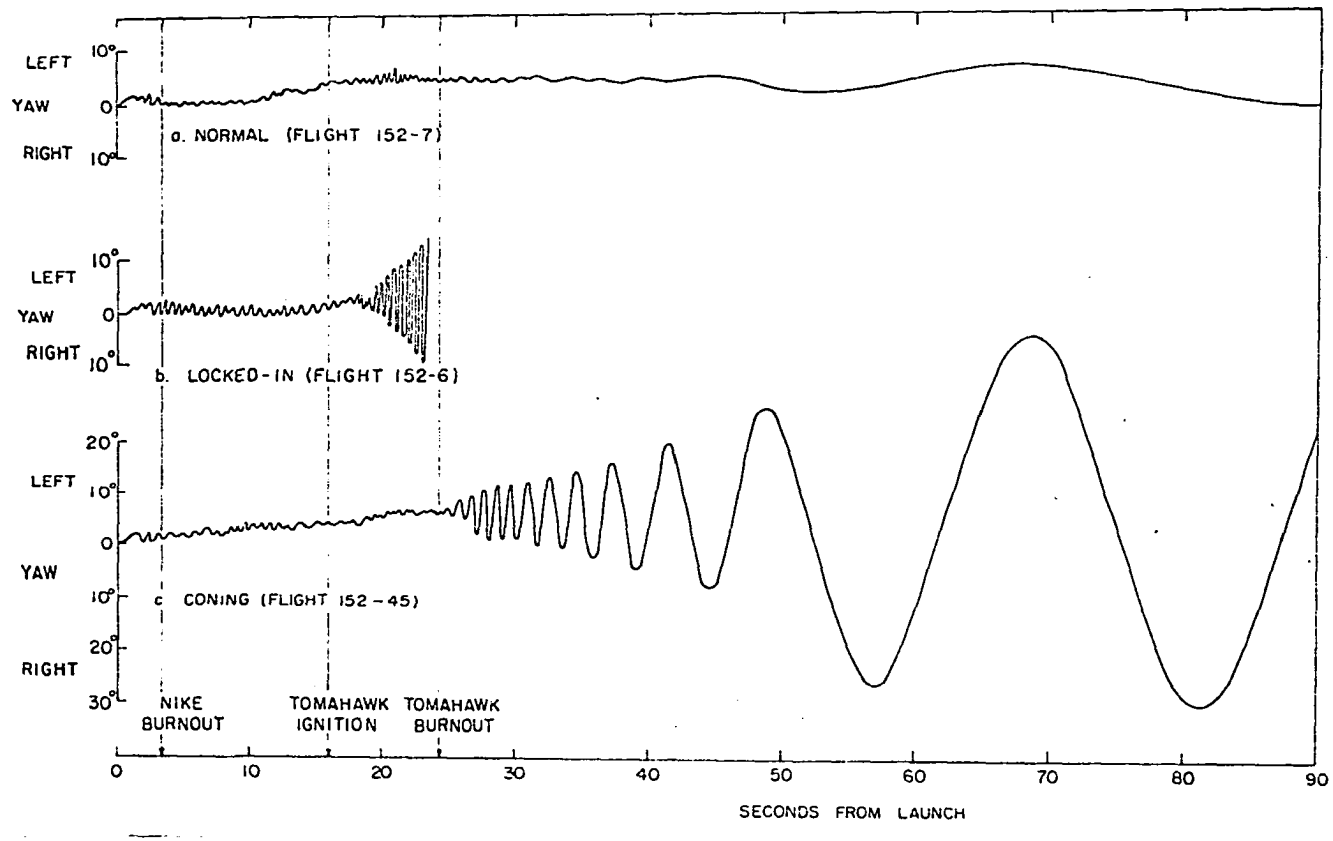

Figure 12 Yaw Gyro Traces from Tomahawk Flights Showing Normal, Locked-In, and Coning Motion. (From Ref. 13)

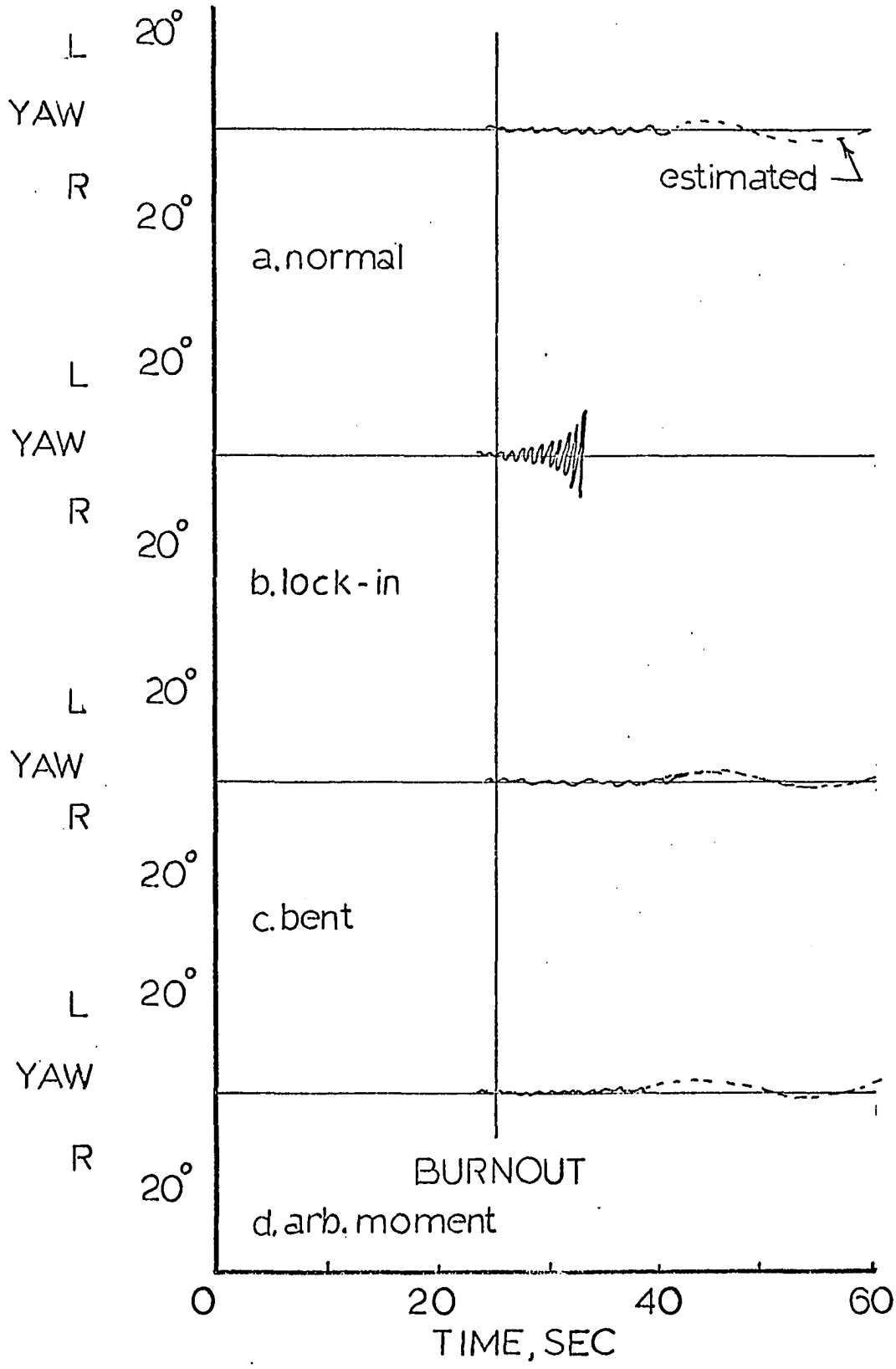

Figure 13 Simulated Yaw Data

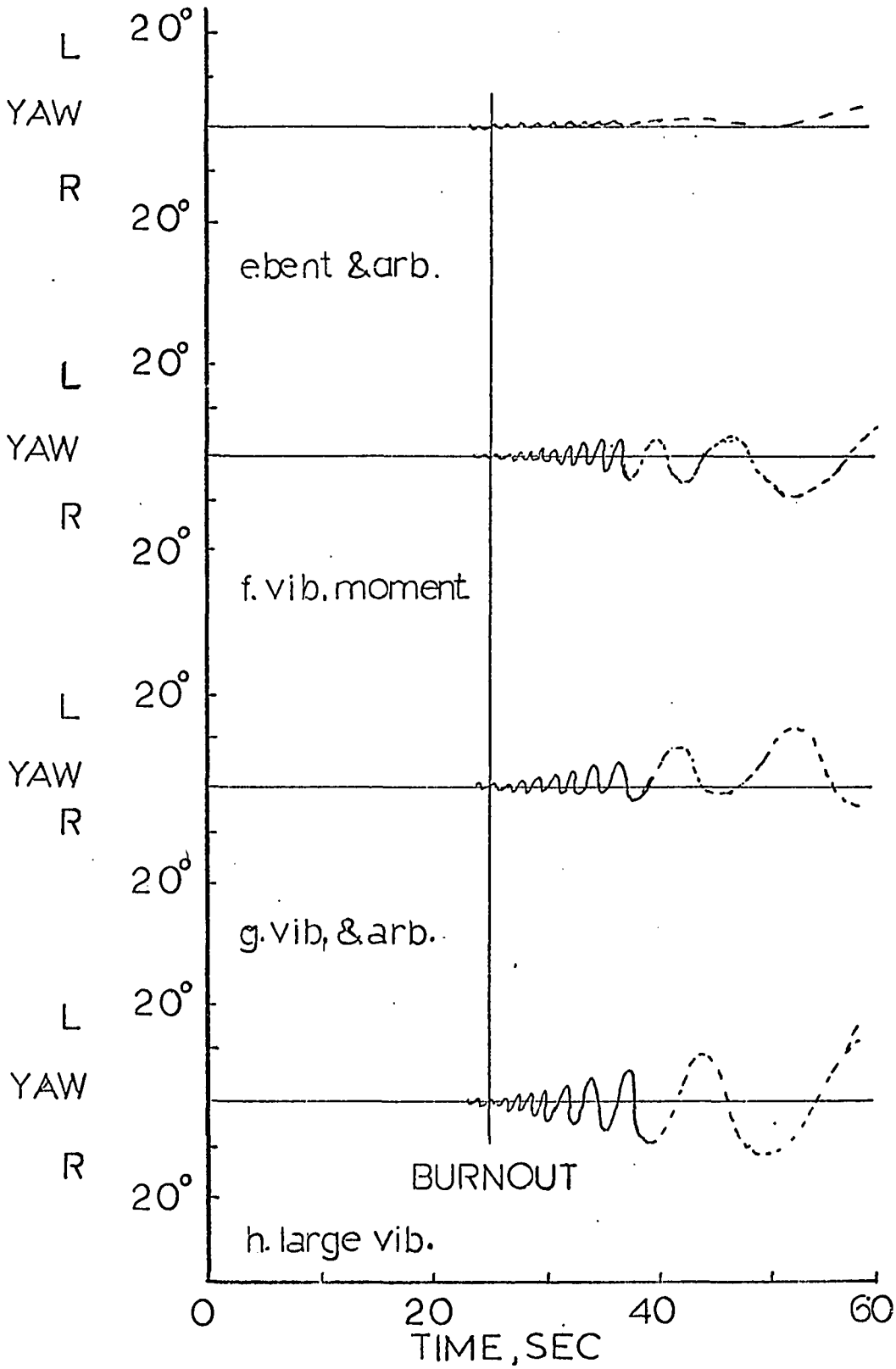

Figure 13 (continued) Simulated Yaw Data

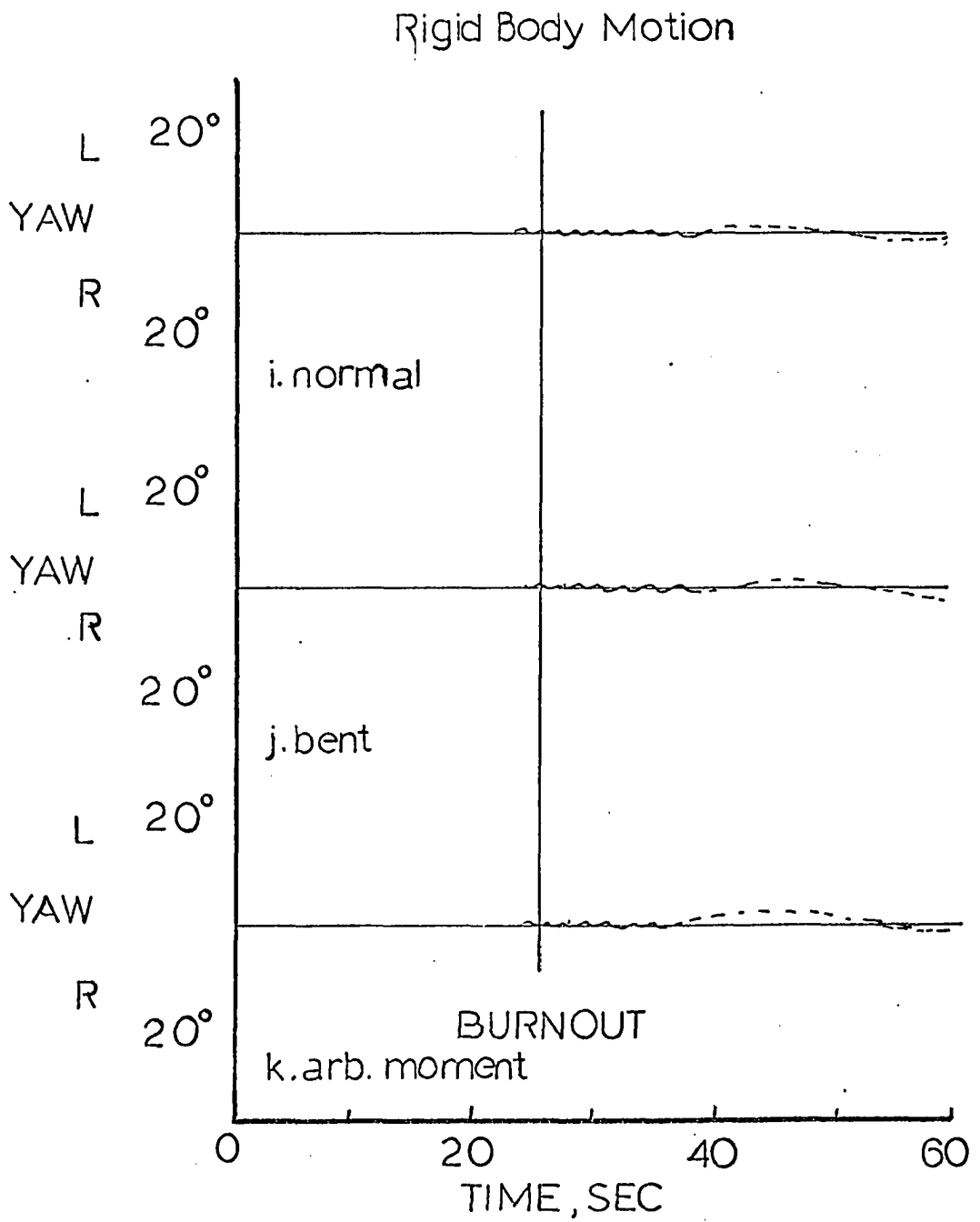

Figure 13 (Continued) Simulated Yaw Data

The difficult motion to simulate is the coning motion. Several different attempts were made to duplicate the motion on the computer. The different cases are as follows:

Case 1. Figure 13c shows the simulated motion of the vehicle with the bent payload moment as the only additional applied moment. Note that the bent payload has very little effect on the total motion of the vehicle.

Case 2. Figure 13d shows the simulated motion of the vehicle with the arbitrary moment applied. Notice that the oscillation tends to drift off from the line of flight but there is little increase in the coning motion.

Case 3. Figure 13e shows the motion caused by applying both the bent payload moment and the arbitrary moment. There is little or no effect on the total motion of the vehicle.

Case 4. The motion of the vehicle was determined using the vibrational moment caused by the continuous vehicle (no loose joint). There was no noticeable difference in the resulting motion for this flight and the normal flight motion. The bent payload moment was applied in addition to the vibrational moment and the resulting motion was identical to that in Case 2.

Case 5. The motion of the vehicle was determined using the vibrational moment caused by the vehicle with a loose payload. Since the payload will bend, the moment caused by the mass offset is also included. Figure 12f shows the resulting motion. The vibrational motion couples with the roll rate, and the yaw angle (and hence the pitch angle) begins to get larger. As the vehicle leaves the atmosphere and no longer has a restoring or damping moment, it can be predicted that the yaw angle will grow to a value of 10-15 degrees. This prediction is based on conservation of angular momentum.

Case 6. Figure 13g shows the motion of the vehicle with the bent payload, its vibrational motion and the arbitrary moment all combined. The motion is simply a superposition of the motion of Case 2 and Case 5. The motion tends to drift off from the line of flight and the yaw angle grows to a predicted 10-15 degrees.

The required flight performance for the Nitehawk 9 (Ref. 3) specifies that the maximum allowable coning angle is ±5 degrees. About one-fourth of the test units failed to meet this requirement by varying amounts. Most of the units that had large coning angles attained angles between ±10 and ±30 degrees. Flight 152-45 shown

in Figure 8a had a coning angle of ± 30 degrees, which was typical. This case does cause coning and does duplicate the smaller coning angle flights. However, it does not account for the larger coning angles.

Case 7. One of the advantages of an analog computer rests in the fact that once the inputs are in the computer, their magnitudes are easily changed. All the input moments were increased to larger values in an attempt to duplicate the larger coning angle flight data. The only duplication obtained occurred when the vibrational input with the loose payload was increased by a factor of four, i.e., the input was changed to $(0.0015 + 0.02 \sin \omega t)$. See Figure 13h.

The motion obtained was virtually identical to the large coning angle flight data. It is an interesting observation but one that is difficult to duplicate in actual flight conditions. The accelerometers flown in most small rockets rockets do not measure data below 50 Hz; therefore, even though the computer simulation duplicates the flight data there is no assurance that such a vibrational environment exists in actual flight. Of course, the magnitude of the vibration may be somewhat greater than those calculated simply because only the thrust induced vibrations were considered. This flexible joint reasoning may further be

strengthened by the fact that the coning has been greatly reduced by stiffening the payload separation joint.

Case 8. In order to determine the effect of reducing the aerodynamic coefficients, function f_1 and function f_2 were reduced in steps. It was found that a 20% reduction in f_1, the restoring moment, did not increase the magnitude of the oscillation angle but did reduce the frequency slightly. However, a 20% reduction in f_2, the damping moment, caused the system to diverge without any disturbing moment.

Case 9. In an attempt to get a complete comparison, the rigid body motions were run on the analog. The rigid body motion was determined using f_1 for rigid body in Figure 10 and the f_2 shown in Figure 11. Figure 13i shows the motion of the rigid vehicle with the standard restoring moments and aerodynamic damping moments. With the same initial conditions as used in the flight shown in Figure 13a, the rigid body motion is almost identical to the normal elastic flight. The final amplitude of the rigid body motion is slightly smaller than the elastic motion and the frequency is different. At two seconds after burnout, the rigid body frequency was 2.5 Hz while the elastic body frequency was 2.75 Hz. The rigid body motion was determined using an applied moment

caused by a bent rocket and the arbitrary moment. These motions are shown in Figures 13j and 13k. It should be noted that these motions are very similar to their corresponding casing in the elastic body motion which are shown in Figures 13c and 13d, respectively. This indicates that the only large effect on the total motion of the vehicle was caused by coupling between the vibrational motion and the yawing motion. Of course, there is no vibrational moment for the rigid body case.

CHAPTER VII

CLOSURE

The integrated approach provides a new and powerful tool for the sounding rocket development engineer. It allows the engineer to determine the effect of various perturbing moments on the oscillatory motion of the vehicle. Furthermore, since the engineer must have a point-mass trajectory, aerodynamic pitching and damping coefficients and an aeroelastic analysis for the basic design of a vehicle, the oscillatory analysis can be done with very little extra effort.

The analysis of the Nitehawk 9 by this method simulates the actual flight data very closely. It showed that the extra-atmospheric coning of the Nitehawk may be caused by the coupling of the vibrational motion with the roll motion. It further showed that variations in the restoring moments had very little effect on the magnitude of oscillations but that the frequency of oscillation was affected; however, lowering the damping moment caused the oscillations to grow.

More investigation is needed in the following areas:

1. A more detailed analysis of the vibrational motion of the vehicle including the thrust induced vibrations, the aerodynamically induced vibrations and the sonically induced vibrations.

2. An analysis to determine the effect created by a payload that is loose enough for the system to react to the forces and moments as a two-body system.

3. An analysis of factors that could cause an instantaneous reduction in the aerodynamic damping.

4. Test and analysis to determine an appropriate magnus moment.

5. Test and analysis to determine an appropriate lee-side vorticity induced moment.

6. Test and analysis to determine the effect of a bent or loose payload on aerodynamic coefficients.

REFERENCES

1. Thomson, K. D., "The Aero-Elastic Divergence of Slender Multi-Stage Test Vehicles," TN-HSA 93, Australian Defense Salisbury, South Australia, November 1962.

2. Reis, G. E. and Sundberg, W. D., "Calculations of the Aeroelastic Bending of a Sounding Rocket Based on Flight Data," Sandia Laboratory (Albuquerque), SC-R-67-1025, March 1967.

3. Womack, W. C., "Nitehawk 9," Sandia Laboratory (Albuquerque), SC-DR-65-456A, January 1966.

4. Stone, G. W., "The Angular Motion of a Rocket-Propelled Vehicle in Free Flight," Sandia Laboratory (Albuquerque), SC-RR-66-42, August 1966.

5. Stone, G. W., "Aerodynamic Analysis of the Sandia Nitehawk 9 Rocket System," Sandia Laboratory (Albuquerque), SC-RR-66-665, February 1966.

6. Prince, L. T., "The Influence of Structural Elasticity on the Stability of Airplanes and Multi-Stage Missiles," AGARD-349, North Atlantic Treaty Organization, Advisory Group for Aeronautical Research and Development, Paris, April 1961.

7. Abraham, L. H., Structural Design of Missile and Spacecraft (New York: McGraw-Hill, 1962).

8. Beal, T. R., "Dynamic Stability of a Flexible Missile Under Constant and Pulsating Thrusts," AIAA Journal, Vol. 3, No. 3, pp. 486-494, March 1965.

9. Meirovitch, L. and Wesley, D. A., "On the Dynamic Characteristics of a Variable-Mass Slender Elastic Body Under High Accelerations," NASA-CR-713, February 1967.

10. Hanson, P. W. and Doggett, R. V., Jr., "Aerodynamic Damping of a 0.02 - Scale Saturn SA-1 Model Vibrating in the First Free-Free Bending Mode," NASA-TN-D-1966, September 1963.

11. Young, Dana, "Generalized Missile Dynamics Analysis II-Equations of Motion," Space Technology Laboratories, GM-TR-0165-359, April 1958.

12. Vaughn, H. R., "A Detailed Development of the Tricyclic Theory," Sandia Laboratories (Albuquerque), SC-M-67-2933, February 1968.

13. Curry, W. H. and Uselton, J. C., "Some Comments on the Aerodynamic Characteristics of the Tomahawk Sounding Rocket," Sandia Corporation, (Albuquerque) SC-R-66-997), March 1967.

14. Muraca, R. J., "An Empirical Method for Determining Static Distributed Aerodynamic Loads on Axismmetric Multistage Launch Vehicles," Langley Research Center, Hampton, Va., NASA TN D-3283, March 1966.

15. Stone, G. W. "Aerodynamic Stability of a Coasting Vehicle Rapidly Ascending Through the Atmosphere," AIAA Journal, Vol. 4, No. 9, pp. 1560-1565, September 1966.

16. Davis, L., Jr.: Follin, J. W., Jr. and Blitzer, Leon, Exterior Ballistics of Rockets (Princeton, N.J.: D. Van Nostrand Company, Inc. 1958).

17. Anonymous, "Six-Degree-of-Freedom Flight-Path Study Generalized Computer Program, Part I - Problem Formulation, "FDL-TDR-64-1, Air Force Flight Dynamics Laboratory, Wright-Patterson Air Force Base, Ohio, 1964.

18. Witte, A. F., "Investigation of Bending Modes in a Single Stage Tomahawk System," Sandia Laboratory (Albuquerque), T-12026, 1966.

19. Fung, Y. C., An Introduction to the Theory of Aeroelasticity (New York: John Wiley & Sons, 1955).

20. Gabrielson, V. K. and Reese, R. T., "SHOCK Code User's Manual - A Computer Code to Solve the Dynamic Response of Lumped-Mass System," Sandia Laboratories (Livermore), SCL-DR-69-98, 1969.

21. Lighthill, M. J., "High Speed Piston Theory Approximation," Journal of Aeronautical Sciences, Vol. 20, p. 402, 1953.

22. Greenwood, D. T., Principles of Dynamics (Englewood Cliffs, N.J.: Prentice-Hall, 1965).

23. Miles, J. W. and Young, Dana, "Generalized Missile Dynamics Analysis III - Aerodynamics," Space Technology Laboratories, GM-TR-0165-00360, April 1958.

APPENDIX A

INTRODUCTION TO THE DERIVATION OF DYNAMICAL EQUATIONS

The purpose of this part of the analysis is to derive the general dynamical equations that govern the motion of an elastic missile in free flight.

The following assumptions are made:

1. The mass of the missile is a function of x only.
2. The lateral bending is governed by Timoshenko beam theory. Even though most sounding rockets are long and slender, the equations are written to include the occasional short missile by including the effects of rotary inertia and shear deformation.
3. The torsional rigidity is assumed to be infinite.
4. The deflections of the missile relative to the moving axes are represented by normal mode oscillations.
5. Structural damping is neglected.

The Coordinate System

Figure 1 shows the general coordinate system. The velocity of the center of mass is denoted by V_o and it is directed along the

tangent to trajectory of the center of mass. The missile configuration is described relative to a set of moving axes (x, y, and z) which has its origin fixed at the center of mass. It is a righthanded orthogonal system that is fixed in the missile body and coincides with the undeflected missile principal axes. The x-axis is directed along the longitudinal axis of symmetry of the undeflected missile*. Displacements along the x axis are denoted by u_1, along the y axis by u_2 and along the z axis by u_3.

The inclination of the x axis from the vertical is denoted by η. Rotation about the x axis is denoted by θ_1 (roll), about the y axis by θ_2 (pitch) and about the z axis by θ_3(yaw). The coordinate system is oriented so that the x-axis is in the trajectory plane.

The Displacement Equations

The displacements can be expressed in the following form:

$$
\begin{aligned}
u_1(x,t) &= c_o(t) + xc_1(t) + \sum_{i=1}^{\infty} \phi_i \cdot q_i(t) \\
u_2(x,t) &= C_o(t) + xc_1(t) + \sum_{j=1}^{\infty} T_j \cdot q_j(t) \\
u_3(x,t) &= k_o(t) + xk_1(t) + \sum_{k=1}^{\infty} \sigma_k \cdot q_k(t)
\end{aligned}
\tag{13}
$$

---

* It can be shown that with this selection of x-axis orientation, the angular momentum of the missile relative to the moving axes is zero.

where ϕ_i, τ_j, σ_k are the eigenfunctions of a free-free beam and q_i, q_j and q_k are the corresponding generalized coordinates. In these expressions, the constants c_o, C_o, k_o, and c_1, C_1, k_1 are parameters that represent rigid-body displacements and rigid-body rotations of the missile relative to the body fixed axes. These parameters are all zero because the axes were chosen such that there is no rigid-body motion relative to the moving axes. Then the equations take the form previously presented as Equations (4). Now considering the corresponding angles of rotation of a missile element, the equations are

$$\psi(x,t) = C_1(t) + \sum_{j=1}^{\infty} \psi_k(x) \cdot q_k(t)$$
$$\Lambda(x,t) = C_1(t) + \sum_{k=1}^{\infty} \lambda_j(x) \cdot q_j(t) \qquad (14)$$

where $C_1(t)$ and $k_1(t)$ are zero as discussed previously. There is no equation for an element rotating about the x axis because of the assumption that the missile is rigid in that plane. This equation takes the form of Equations (5).

The Derivation of the Kinematic Relations for Velocities from Figure 2.

$$\overline{P} = \overline{R} + \overline{\rho}\ ; \quad \rho = (x + u_1)\overline{i} + (y + u_2)\overline{j} + (z + u_3)\overline{k} \qquad (15)$$

$$\dot{\overline{P}} = \dot{\overline{R}} + \dot{\overline{\rho}} = \dot{\overline{R}} + (\dot{x} + \dot{u}_1)\overline{i} + (x + u_1)\dot{\overline{i}} + (\dot{y} + \dot{u}_2)\overline{j} + (y + u_2)\dot{\overline{j}} + (\dot{z} + \dot{u}_3)\overline{k} + (z + u_3)\dot{\overline{k}} \qquad (16)$$

From Greenwood (Ref. 22)

$$\dot{\bar{i}} = \dot{\theta}_3 \bar{j} - \dot{\theta}_2 \bar{k} \; ; \quad \dot{\bar{j}} = \dot{\theta}_1 \bar{k} - \dot{\theta}_3 \bar{i} \; ; \quad \dot{\bar{k}} = \dot{\theta}_2 \bar{i} - \dot{\theta}_1 j \tag{17}$$

Then the velocity can be written

$$\dot{\bar{P}} = \dot{\bar{R}} + (\dot{x} + \dot{u}_1)\bar{i} + (\dot{y} + u_2)\bar{j} + (\dot{z} + u_3)\bar{k} + (x + u_1)(\dot{\theta}_3 j - \dot{\theta}_2 \bar{k})$$

$$+ (y + u_2)(\dot{\theta}_1 \bar{k} - \dot{\theta}_3 \bar{i}) + (z + u_3)(\dot{\theta}_2 \bar{i} - \dot{\theta}_1 \bar{j}) \tag{18}$$

Then noting that $\dot{x} = \dot{y} = \dot{z} = 0$ because the coordinate system is body-fixed, the velocity becomes

$$\dot{\bar{P}} = \dot{\bar{R}} + [\dot{u}_1 - (y + u_2)\dot{\theta}_3 + (z + u_3)\dot{\theta}_2]\bar{i} + [\dot{u}_2 + (x + u_1)\dot{\theta}_3 - (z + u_3)\dot{\theta}_1]\bar{j}$$

$$+ [\dot{u}_3 - (x + u_1)\dot{\theta}_2 + (y + u_2)\dot{\theta}_1]\bar{k} \tag{19}$$

Then the absolute velocities are

$$V_x = \dot{R}_x + [\dot{u}_1 - (y + u_2)\dot{\theta}_3 + (z + u_3)\dot{\theta}_2]$$

$$V_y = \dot{R}_y + [\dot{u}_2 + (x + u_1)\dot{\theta}_3 - (z + u_3)\dot{\theta}_1] \tag{20}$$

$$V_z = \dot{R}_z + [\dot{u}_3 - (x + u_1)\dot{\theta}_2 + (y + u_2)\dot{\theta}_1]$$

Accelerations from Figure 2

The velocity components of the center of mass can be expressed in terms of the flight-path velocity and coordinates in the following manner.

$$\dot{R}_x = V_o \cos\alpha \; , \qquad \dot{R}_y = V_o \cos\beta \; , \qquad \dot{R}_z = V_o \sin\alpha \tag{21}$$

It should be noted that the total angular rotation of a point on the missile axis is not simply θ_2 about the y axis and θ_3 about the z axis. Making a small-angle assumption, the rotation in the pitch plane (xz plane) is $\theta_2 + \partial u_3/\partial x$ and the rotation in the yaw plane (xy plane) is $\theta_3 + \partial u_2/\partial x$. Therefore, the total pitch angle of attack is not $\alpha = \gamma - \theta_2$ but $\alpha_T = \gamma - \theta_2 - \partial u_3/\partial x$. The total yaw angle of attack is $\beta = \theta_3 + \partial u_2/\partial x$. The acceleration components of the center of mass can now be written in terms of the flight path velocity and coordinates as:

$$
\begin{aligned}
\ddot{R}_x &= \dot{V}_o \cos\alpha - V_o \dot{\alpha} \sin\alpha & \alpha &= \alpha - \theta_2 \\
\bar{A}_x &= \dot{V}_o \cos\alpha - V_o \dot{\gamma} \sin\alpha & \dot{\alpha} &= \dot{\gamma} \\
\ddot{R}_y &= \dot{V}_o \cos\beta - V_o \dot{\beta} \sin\beta & \beta &= \theta_3 + \partial u_2/\partial x \\
\bar{A}_y &= \dot{V}_o \cos\beta - V_o \theta_3 \sin\beta & & \\
\ddot{R}_z &= \dot{V}_o \sin\alpha + V_o \dot{\alpha} \cos\alpha & \beta &= \theta \\
\bar{A}_z &= \dot{V}_o \sin\alpha \quad V_o \dot{\gamma} \cos\alpha & &
\end{aligned}
\qquad (22)
$$

Derivation of the Kinetic Energy of the System

The kinetic energy associated with the velocity of points along the missile axis is:

$$T_L = \frac{1}{2} \int_{-\ell_1}^{\ell_2} (V_x^2 + V_y^2 + V_z^2)\, dm$$

$$= \frac{1}{2} \int_{-\ell_1}^{\ell_2} \Big\{ \Big[\dot{R}_x + \dot{u}_1 - (y + u_2)\dot{\theta}_3 + (z + u_3)\dot{\theta}_2\Big]^2 \tag{23}$$

$$+ \Big[\dot{R}_y + \dot{u}_2 + (x + u_1)\dot{\theta}_3 - (z + u_3)\dot{\theta}_1\Big]^2$$

$$+ \Big[\dot{R}_z + \dot{u}_3 - (x + u_1)\dot{\theta}_2 + (y + u_2)\dot{\theta}_1\Big]^2 \Big\}\, dm$$

Now consider the kinetic energy due to the rotary inertia of each infinitesimal transverse slice of the missile. The angular velocity of any slice is given by the rigid-body (θ_2, θ_3) rotational velocity and the rotational velocity associated with bending ($\dot{\Psi}, \dot{\Lambda}$). The corresponding kinetic energy is

$$T_R = \frac{1}{2} \int_{-\ell_1}^{\ell_2} \Big[r^2(\theta_2 + \Psi)^2 + r^2(\theta_3 + \Lambda)^2\Big]\, dm \tag{24}$$

where r is the radius of gyration of each element. Angles Ψ and Λ are defined in the derivation of the deflection equations. The total kinetic energy is

$$T_T = T_L + T_k \tag{25}$$

The Equations of Rotation

The Lagrangian equation for some rotation is

$$\frac{d}{dt}\left(\frac{\partial T}{\partial \dot{\xi}}\right) - \frac{\partial T}{\partial \xi} = Q_\xi \tag{26}$$

The kinetic energy of the system was shown to be

$$\begin{aligned} T_T = \int_{-\ell_1}^{\ell_2} \Big\{ & \left[\dot{R}_x + \dot{u}_1 - (y + u_2)\dot{\theta}_3 + (z + u_3)\dot{\theta}_2\right]^2 \\ & + \left[\dot{R}_y + \dot{u}_2 + (x + u_1)\dot{\theta}_3 - (z + u_3)\dot{\theta}_1\right]^2 \\ & + \left[\dot{R}_z + \dot{u}_3 - (x + u_1)\dot{\theta}_2 + (y + u_2)\dot{\theta}_1\right]^2 \Big\} dm \\ & + \frac{1}{2}\int_{-\ell_1}^{\ell_2} \left[r^2(\dot{\theta}_2 + \dot{\Psi})^2 + y^2(\dot{\theta}_3 + \dot{\Lambda})^2 \right] dm \end{aligned} \tag{27}$$

The Langrangian equation for θ_2 is:

$$\begin{aligned} \frac{\partial T}{\partial \theta_2} = \int_{-\ell_1}^{\ell_2} \Big\{ & \left[\dot{R}_x + \dot{u}_1 - (y + u_2)\dot{\theta}_3 + (z + u_3)\dot{\theta}_2\right](z + u_3) \\ & + \left[\dot{R}_z + \dot{u}_3 + (x + u_1)\dot{\theta}_2 + (y + u_2)\dot{\theta}_1\right](x + u_1) \Big\} dm \\ & + \int_{-\ell_1}^{\ell_2} r^2(\dot{\theta}_2 + \dot{\Psi})^2(1)\, dm \end{aligned}$$

or

$$\frac{\partial T}{\partial \theta_2} = \int_{-\ell_1}^{\ell_2} \Big\{ \Big[\dot{R}_x(z + u_3) + \dot{u}_1(z + u_3) - (yz + u_2 z + u_3 y + u_2 u_3)\dot{\theta}_3 + (z^2 + 2u_3 z + u_3^2)\dot{\theta}_2 \Big] + \Big[\dot{R}_z(x + u_1) + (x + u_1)\dot{u}_3 + (x^2 + 2u_1 x + u_1^2)\dot{\theta}_2 + (xy + u_2 x + u_1 y + u_2 u)\dot{\theta}_1 \Big] \Big\} dm + \int_{-\ell_1}^{\ell_2} r^2(\dot{\theta}_2 + \dot{\psi})\, dm \tag{28}$$

Terms of the form $\dot{R}_x \int u_3 dm$, $\dot{u}_1 \int u_3 dm$, and $r^2 \int \dot{\psi}\, dm$ vanish because of properties of the eigenfunctions and terms like $u_3 \quad y\, dm$ vanish because the origin of the coordinate system is at the center of mass. Then, Equation (28) becomes

$$\frac{\partial T}{\partial \dot{\theta}_2} = \int_{-\ell_1}^{\ell_2} \Big[-yz\dot{\theta}_3 + (z^2 + u_3^2)\dot{\theta}_2 + (x^2 + u_1^2)\dot{\theta}_2 + xy\dot{\theta}_1 \Big] dm + \int_{-\ell_1}^{\ell_2} r^2\, \dot{\theta}_2\, dm$$
$$= I\dot{\theta}_2\dot{\theta}_2 + \int_{-\ell_1}^{\ell_2} (-xz\dot{\theta}_3 + xy\dot{\theta}_1)\, dm \tag{29}$$

where

$$I_{\theta_2} = \int_{-\ell_1}^{\ell_2} (z^2 + x^2 + u_3^2 + u_1^2 + r^2)dm \tag{30}$$

The term $\partial T/\partial \theta_2$ vanishes in this case because the kinetic energy equation is independent of θ_2.

The generalized force Q_{θ_2} equals the moment about the center of mass of all the external forces that produce work during a vertical displacement $\Delta\theta_2$. From Figure 3

$$Q_{\theta_2} = J_{Dz}\ell_1 - Tu_{3T}' + T\theta_{2T} + M_{\theta_2}^* \tag{31}$$

where $M_{\theta_2}^*$ is the moment about the center of mass during the angular displacement $\Delta\theta_2$. Then the Lagrangian equation becomes

$$\frac{d}{dt}\left[I_{\theta_2}\dot{\theta}_2 + \int_{-\ell_1}^{\ell_2}(-yz\theta_3 + xy\theta_1)dm\right] = J_{Dz}\ell_1 - T^*u'_{3T}\ell_1 + T^*u_{3T} + M^*_{\theta_2}$$

or

$$\frac{d}{dt}\left(I_{\theta_2}\dot{\theta}_2\right) + \int_{-\ell_1}^{\ell_2}\left(-\dot{y}z\dot{\theta}_3 - y\dot{z}\dot{\theta}_3 - xz\ddot{\theta}_3 + \dot{x}y\dot{\theta}_1 + x\dot{y}\dot{\theta}_1 + xy\ddot{\theta}_1\right)dm$$

$$= J_{Dz}\ell_1 - T^*u'_{3T}\ell_1 + T^*u_{3T} + M^*_{\theta_2} \tag{32}$$

Terms such as $-\int(xz - xz)dm$ are recognized as angular momentum terms.

The terms $\ddot{\theta}_3\int xz\,dm$ and $\ddot{\theta}_1\int xy\,dm$ vanish because the coordinate axis is along the principal axis of the body. Then equation (32) becomes

$$\frac{d}{dt}\left(I_{\theta_2}\dot{\theta}_2\right) + (I_{xx} - I_{zz})\dot{\theta}_1\dot{\theta}_3 = (J_{Dz} - T^*u'_{3T})\ell_1 + T^*u_{3T} + M^*_{\theta_2} \qquad (33)$$

where $(y\dot{z} - \dot{y}z)dm = I_{xx}\dot{\theta}_1$

$(\dot{x}z - x\dot{z})dm = I_{yy}\dot{\theta}_2$

$(x\dot{y} - \dot{x}y)dm = I_{zz}\dot{\theta}_3$

The expression for I_{θ_2} is the instantaneous mass amount of inertia because the configuration of the missile changes with respect to the axes. However, in the practical situation, this variation will be small compared to the total. The approximation generally used is that the moment of inertia is independent of time and equal to

$$\therefore \quad I_{yy} = \int_{-\ell_1}^{\ell_2} (z^2 + x^2)\, dm \qquad (34)$$

With this assumption, the Lagrangian equation becomes

$$I_{yy}\ddot{\theta}_2 + (I_{xx} - I_{zz})\dot{\theta}_1\dot{\theta}_3 = J_{Dz}\ell_1 - T^*u'_{3T}\ell_1 + T^*u_{3T} + M^*_{\theta_2} \qquad (35)$$

The Lagrangian equation for θ_3 is derived in a similar manner.

$$Q_{\theta_3} = J_{Dy}\theta_1 - Tu'_{2T}\ell_1 + Tu_{2T} + M^*_{\theta_3} \qquad (36)$$

Then the Lagrangian equation becomes

$$\frac{d}{dt}\left[I_{\theta_3}\dot{\theta}_3 + \int_{-\ell_1}^{\ell_2} (-yz\dot{\theta}_2 - xz\dot{\theta}_1)\, dm\right] = (J_{Dy} - Tu_{2T})\ell_1 + Tu_{2T} + M^*_{\theta_3} \qquad (37)$$

Making the same assumption as for I_{θ_2}.

$$I_{\theta_3} \doteq I_{zz} = \int_{-\ell_1}^{\ell_2} (x^2 + y^2)\, dm \tag{38}$$

Because of the axial symmetry of most sounding rockets, the moments of inertia I_{zz} and I_{yy} are equal. In a manner similar to the θ_2 equation, this equation reduces to

$$I_{zz}\ddot{\theta}_3 + (I_{yy} - I_{xx})\dot{\theta}_1\dot{\theta}_2 = (J_{Dy} - Tu'_{2T})\ell_1 + Tu_{2T} + M^*_{\theta_3} \tag{39}$$

The one remaining rotation equation is the roll equation. In this case

$$\frac{\partial T}{\partial \dot{\theta}_1} = \int_{-\ell_1}^{\ell_2} \left\{ \left[\dot{R}_y + \dot{u}_2 + (x + u_1)\dot{\theta}_3 - (z + u_3)\dot{\theta}_1 \right] \left[-(z + u_3) \right] \right.$$

$$\left. + \left[\dot{R}_z + \dot{u}_3 + (x + u_1)\dot{\theta}_2 + (y + u_2)\dot{\theta}_1 \right] \left[y + u_2 \right] \right\} \tag{40}$$

With the previous assumptions, this becomes

$$\frac{\partial T}{\partial \dot{\theta}_1} = \int_{-\ell_1}^{\ell_2} \left[-xz\dot{\theta}_3 + (z^2 + u_3^2)\dot{\theta}_1 + xy\dot{\theta}_2 + (y^2 + u_2^2)\dot{\theta}_1 \right] dm$$

or

$$\frac{\partial T}{\partial \dot{\theta}_1} = I_{\theta_1}\dot{\theta}_1 + \int_{-\ell_1}^{\ell_2} (-xz\dot{\theta}_3 + xy\dot{\theta}_2)\, dm \tag{41}$$

where

$$I_{\theta_1} = \int_{-\ell_1}^{-\ell_2} (y^2 + z^2 + u_2^2 + u_3^2)\, dm \tag{42}$$

Since the kinetic energy is not a function of θ_1,

$$\partial T/\partial \theta_1 = 0. \tag{43}$$

The generalized force is the moment acting about the x axis. The x axis is assumed to be the roll axis and the only moment acting is the aerodynamic roll moment, $M^*_{\theta_1}$.

Then the Lagrangian equation becomes

$$\frac{d}{dt}\left[I_{\theta_1}\dot{\theta}_1 + \int_{-\ell_1}^{\ell_2} (-xz\dot{\theta}_3\ xy\dot{\theta}_2)\, dm\right] = M^*_{\theta_1} \tag{44}$$

Using the previous assumption and recognizing the angular momentum terms, Equation (44) becomes

$$I_{xx}\ddot{\theta}_1 + (I_{zz} - I_{yy})\dot{\theta}_2\dot{\theta}_3 = M^*_{\theta_1} \tag{45}$$

But sounding rockets are generally axially symmetric and dynamically balanced, so $I_{zz} = I_{yy}$. Therefore, Equation (45) reduces to

$$I_{xx}\ddot{\theta}_1 = M^*_{\theta_1} \tag{46}$$

Motion of the Center of Mass

Using Newton's second law and referring to Figure 3, one obtains the equations of motion for the center of mass

$$M(x)\,\bar{A}_x = T - Mg\cos\eta + F_x^*$$

$$M(x)\,\bar{A}_y = Tu'_{2T} + F_y^* - J_{Dy} \qquad (47)$$

$$M(x)\,\bar{A}_z = Tu'_{3T} + Mg\sin\eta - J_{Dz} + F_z^*$$

In the derivation of these equations, the angle of inclination from the vertical, η, is assumed to be small. Therefore, T in the x equation is assumed to be directed along the x axis, u'_{2T} is the slope of the displacement in the y direction at the tail of the missile and is, therefore, approximately equal to the angle of deflection, u'_{3T} is the slope in the z direction.

The resultant aerodynamic forces in the x, y and z direction are F_x^*, F_y^*, and F_z^*. Here F_x^* is approximately equal to the negative of the drag; F_y^* and F_z^* are approximately equal to the normal force in the xy and xz plane; J_{Dy} and J_{Dz} are the jet damping forces in the xy and xz planes. The normal forces in the xy and xz planes are actually distributed forces but these forces are not well defined for large Mach numbers. Miles and Young (Ref. 23) showed in their report that the slender body approximation is very sensitive to discontinuities in missile body slope and the approximation is not accurate for Mach numbers above two. An approximation that is valid at high Mach numbers and that is at least less sensitive to discontinuities in slope is the piston-theory approximation developed

by Lighthill (Ref. 21). However, this approximation requires careful definition of local parameters such as local velocity and local downwash. Sounding-rocket design methods have not yet reached that degree of sophistication. It is common practice in the sounding rocket field to determine a distributed load using a semi-empirical method described in Reference 14 and then correcting the load to correspond to wind tunnel data. This method is described in Appendix C. Since actual flight data and wind tunnel data are available, the method described in Ref. 14 will be used in this analysis.

The Derivation of the Bending Equations

The Lagrangian equation for a normal bending mode is

$$\frac{d}{dt}\left(\frac{\partial T}{\partial \dot{q}_n}\right) - \frac{\partial T}{\partial q_n} + \frac{\partial V}{\partial q_n} = Q_{qn} \tag{48}$$

Now to find the parts of the equation in the u_3 direction

$$\frac{\partial T}{\partial \dot{q}_k} = \int_{-\ell_1}^{\ell_2} \left\{\left(\dot{R}_z + \dot{u}_3 - (x + u_1)\dot{\theta}_2 + (y + u_2)\dot{\theta}_1\right)\frac{\partial \dot{u}_3}{\partial \dot{q}_k}\right. dm$$

$$\left. + \frac{2}{2}\int_{-\ell_1}^{\ell_2} r^2(\dot{\theta}_2 + \dot{\psi})\,\frac{\partial \psi}{\partial q_k}\right. \tag{49}$$

From the deflection equations,

$$u_3(x,t) = \sum_{k=1}^{\infty} \sigma_k(x) \cdot q_k(t) \qquad \Psi = \sum_{j=1}^{\infty} \psi_k(x) \cdot q_k(t)$$

$$\dot{u}_3 = \sigma_k \cdot \dot{q}_k \qquad \Psi = \psi_k \dot{q}_k \tag{50}$$

$$\partial \dot{u}_3/\partial \dot{q}_i = \sigma_k \qquad \partial \Psi/\partial q_{qi} = \psi_k$$

then

$$\partial T/\partial q_i = \int_{-\ell_1}^{\ell_2} \left[R_2 + u_3 - (x + u_1)\dot{\theta}_2 + (y + u_2)\dot{\theta}_1 \; q_k \right] dm$$

$$+ \int_{-\ell_1}^{\ell_2} r^2(\dot{\theta}_2 + \dot{\psi})_k \, dm \tag{51}$$

This expression can be simplified by using the properties of the eigenfunctions given in a separate section.

Breaking the integrals into parts, it can be seen that

$$\dot{R}_z \int_{-\ell_1}^{\ell_2} \sigma_k dm = 0 , \quad u_2\theta_1 \int_{-\ell_1}^{\ell_2} \sigma_k \, dm = 0 , \quad u_1\dot{\theta}_2 \int_{-\ell_1}^{\ell_2} \sigma_k \, dm = 0$$

$$r^2\dot{\theta}_2 \int_{-\ell_1}^{\ell_2} \psi_k \, dm = 0 , \quad \int_{-\ell_1}^{\ell_2} x \, dm = \int_{-\ell_1}^{\ell_2} y \, dm = 0 \tag{52}$$

Thus, the only terms left are

$$\int_{-\ell_1}^{\ell_2} (\dot{u}_3 \sigma_k + r^2 \dot{\psi}\, \psi_k)\, dm \tag{53}$$

Then from the displacement equation,

$$\int_{-\ell_1}^{\ell_2} \left[(\sigma_k \cdot \dot{q}_k)\, \sigma_k + (r^2 \psi_k q_k)\, \psi_k \right] dm$$

$$= \dot{q}_i \int_{-\ell_1}^{\ell_2} \left[\sigma_k \cdot \sigma_k + r^2\, \psi_k \psi_k \right] dm = q_i\, M \tag{54}$$

Therefore

$$\partial T / \partial \dot{q}_k = \dot{q}_k M \tag{55}$$

where M is the total mass.

In a similar manner, the vibration in the xy plane yields

$$\partial T / \partial q_i = \dot{q}_j M \tag{56}$$

Now to find $\partial T / \partial q_n$ for the u_3 direction,

$$\partial T / \partial q_k = \int_{-\ell_1}^{\ell_2} \left\{ \left[\dot{R}_y + \dot{u}_1 - (y + u_2)\dot{\theta}_3 + (z + u_3)\dot{\theta}_2 \right] (\dot{\theta}_2)\, \frac{\partial u_3}{\partial q_k} \right.$$

$$\left. + \left[\dot{R}_y + \dot{u}_2 + (x + u_1)\dot{\theta}_3 - (z + u_3)\dot{\theta}_1 \right] \left[(-\dot{\theta}_1) \frac{\partial u_3}{\partial q_k} \right] \right\} dm \tag{57}$$

Now

$$\frac{\partial u_3}{\partial q_k} = \sigma_k \tag{58}$$

Then

$$\partial T/\partial q_i = \int_{-\ell_1}^{\ell_2} \left[\dot{R}_x \dot{\theta}_2 - u_2 \dot{\theta}_2 \dot{\theta}_3 + u_3 \dot{\theta}_2^2 - R_y \dot{\theta}_1 - \dot{u}_2 \dot{\theta}_1 - u_1 \dot{\theta}_1 \dot{\theta}_3 + u_3 \dot{\theta}_1^2\right] \sigma_k \, dm \tag{59}$$

In the previous section it was shown that all the terms vanish except two. That is

$$\begin{aligned} \partial T/\partial q_i &= \int_{-\ell_1}^{\ell_2} (u_3 \dot{\theta}_2^2 + u_3 \dot{\theta}_1^2) \, \sigma_k \, dm \\ &= \dot{\theta}_2^2 \int_{-\ell_1}^{\ell_2} u_3 \sigma_k dm + \dot{\theta}_1^2 \int_{-\ell_1}^{\ell_2} u_3 \sigma_k \, dm \end{aligned} \tag{60}$$

The sum of these two terms must be zero in order to be consistent with the assumption that the vibrational motions take place in normal modes in two independent planes. In like manner, $\partial T/\partial q_j$ is assumed to be zero.

From beam theory, the potential energy V is the elastic strain energy due to bending and transverse shear, that is,

$$V = \frac{1}{2}\int_{-\ell_1}^{\ell_2} EI\left(\frac{\partial \psi_i}{\partial x}\right)^2 dx + \frac{1}{2}\int_{-\ell_1}^{\ell_2} K_1 AG\left(\frac{\partial \phi_i}{\partial x} - \psi_i\right)^2 dx \qquad (61)$$

where these terms are defined in the properties of eigenfunctions.

The xz plane equations are derived as follows:

$$u_3(x,t) = \sum_{k=1}^{\infty} \sigma_k(x) \cdot q_k(t) \qquad \psi(x,t) = \sum_{k=1}^{\infty} \psi_k(x) \cdot q_k(t) \qquad (62)$$

Then

$$V_{xz} = \frac{1}{2}\int_{-\ell_1}^{\ell_2} EI \frac{\partial \psi_k}{\partial x} q_k \frac{\partial \sigma_k}{\partial x} q_k \, dx + \frac{1}{2}\int_{-\ell_1}^{\ell_2} KAG\left(\frac{\partial \sigma_k}{\partial x} q_k - \psi_{kq_k}\right)^2 dx \qquad (63)$$

By relations of eigenfunctions

$$V_{xz} = \frac{1}{2} M \sum_{k=1}^{\infty} \omega_k^2 q_k^2 \qquad (64)$$

In a similar manner, the potential energy in the xy plane is

$$V_{xy} = \frac{1}{2} M \sum_{j=1}^{\infty} \omega_j^2 q_j^2 \qquad (65)$$

From these

$$\frac{\partial V_{xz}}{\partial q_k} = M\omega_k^2 q_k \qquad \frac{\partial V_{xy}}{\partial q_k} = M\omega_j^2 q_j \qquad (66)$$

Now the generalized force in the xz plane is

$$Q_{xz} = \int_{-\ell_1}^{\ell_2} P_{xz}(x,t) \cdot \frac{\partial u_3}{\partial q_k}\, dx + T\, u_{3T}' \left(\frac{\partial u_3}{\partial q_k}\right)_{x=-\ell_1} \tag{67}$$

$$\frac{\partial u_3}{\partial q_k} = \sigma_k(x) \quad \left(\frac{\partial u_3}{\partial q_k}\right)_{x=-\ell_1} = \sigma_k(-\ell_1)$$

Then

$$Q_{xz} = \int_{-\ell_1}^{\ell_2} P_{xz}(x,t)\, \sigma_k(x)\, dx + T\, u_3'\, \sigma_k(-\ell_1) \tag{68}$$

In a similar manner,

$$Q_{xy} = \int_{-\ell_1}^{\ell_2} P_{xy}(x,t)\ T_j(x)\, dx + T\, u_2'\, T_j(-\ell_1) \tag{69}$$

Now substitute all of this back into the general Lagrangian equation.

For xz plane,

$$\frac{d}{dt}\ (\dot{q}_k M) + M\, \omega_k^2 q_k = \int_{-\ell_1}^{\ell_2} P_{xz}(x,t)\, \sigma_k(x)\, dx + T^* u_3'\, \sigma_k(-\ell_1) \tag{70}$$

$$M(\ddot{q}_k + \omega_k^2 q_k) = \int_{-\ell_1}^{\ell_2} P_{xz}(x,t)\, \sigma_k(x)\, dx + T^* u_3'\, \sigma_k(-\ell_1)$$

Then, in the xy plane,

$$M(\ddot{q}_j + \omega_j^2 q_j) = \int_{-\ell_1}^{\ell_2} P_{xy}(x,t)\ T_j(x)\, dx + T^* u_2'\, T_j(-\ell_1) \tag{71}$$

Properties of Eigenfunctions

The properties of the eigenfunctions are determined in the same manner as used in Reference 11. Considering a Timoshenko beam, let ω_i = circular frequency of the ith mode, $\phi_i(x)$ = eigenfunction representing total deflection (due to both bending and shear) of the ith mode, $\psi_i(x)$ = eigenfunction representing the slope due to bending alone of the ith mode.

The following assumptions are made

1. The missile is treated as a free-free beam with a total length of $\ell_1 + \ell_2$.
2. The eigenfunctions are normalized so that

$$\int_{-\ell_1}^{\ell_2} (\phi_i^2 + r^2\psi_i^2)\, dm = 0.$$

Then the eigenfunctions for a free-free beam satisfy the following mathematical relations that are necessary for this analysis.

$$\int_{-\ell_1}^{\ell_2} (\phi_i \phi_n + r^2\psi_i\psi_n)\, dm = \begin{bmatrix} 0 \text{ for } n \neq i \\ M \text{ for } n = i \end{bmatrix} \tag{72}$$

$$\int_{-\ell_1}^{\ell_2} EI \frac{d\psi_i}{dx} \cdot \frac{d\psi_n}{dx}\, dx + \int_{-\ell_1}^{\ell_2} K_1 AG \left(\frac{d\phi_n}{dx} - \psi_1\right)$$

$$\left(\frac{d\phi_n}{dx} - \psi_n\right) dx = \begin{bmatrix} 0 \text{ for } n \neq i \\ M\omega_i^2 \text{ for } n = i \end{bmatrix} \qquad (73) \text{ Cont.}$$

$$-\int_{-\ell_1}^{\ell_2} \phi_i \, dm = 0$$

$$-\int_{-\ell_1}^{\ell_2} (x\phi_i + r^2\psi_i) \, dm = 0$$

where $i = 1, 2, 3 \ldots$, $n = 1, 2, 3 \ldots$, and K_1AG = shearing stiffness.

APPENDIX B

TRANSFORMATION OF EQUATIONS INTO AEROBALLISTIC REFERENCE SYSTEM

The equations derived in Appendix A are expressed in a body-fixed coordinate system. In order to compare the angular motion obtained from the equation with flight data, the equations of motion will be transformed to the reference system used while gathering the flight data. This reference system is often called the "Aeroballistic Reference System". The aeroballistic reference system is a system of axes that are fixed at the center of mass of the rocket and that pitches and yaws with the body but does not roll with the body. Figure 4 shows the axes system attached to the body. The equations will be transformed in a manner suggested in Ref. 12.

The equations derived in Appendix A can be expressed in matrix form as follows:

$$\begin{pmatrix} M^{*}_{\theta_1} \\ M^{*}_{\theta_2} \\ M^{*}_{\theta_3} \end{pmatrix} = \begin{bmatrix} I_{xx} & 0 & 0 \\ 0 & I_{yy} & 0 \\ 0 & 0 & I_{zz} \end{bmatrix} \begin{pmatrix} \ddot{\theta}_1 \\ \ddot{\theta}_2 \\ \ddot{\theta}_3 \end{pmatrix} + \begin{pmatrix} \dot{\theta}_1 \\ \dot{\theta}_2 \\ \dot{\theta}_3 \end{pmatrix} \begin{bmatrix} I_{xx} & 0 & 0 \\ 0 & I_{yy} & 0 \\ 0 & 0 & I_{zz} \end{bmatrix} \quad (74)$$

When the matrix algebra is completed, this equation provides the three moment equations for a body-fixed axis system. For the aeroballistic system, substitute r for θ to identify the different forms of the equations. Then in the aeroballistic system, r_1 is made zero in the matrix since it is a non-rolling axis system. Rewritten in terms of aeroballistic axes, the equations become:

$$
\begin{aligned}
I_{xx}\,\ddot{r}_1 &= M^*_{r_1} \\
I_{yy}\,\ddot{r}_2 + \dot{r}_1 \dot{r}_3\, I_{xx} &= M^*_{r_2} \\
I_{zz}\,\ddot{r}_3 - \dot{r}_2 \dot{r}_1\, I_{xx} &= M^*_{r_3}
\end{aligned}
\tag{75}
$$

APPENDIX C

CALCULATION OF THE APPLIED LOADS AND MOMENTS

General

The approach to the calculation of the aerodynamic loads and moments is to use methods and tools that are in common use among sounding rocket developers. This approach allows quite a variation in the degree of sophistication in the technique used for the different loads and moments. In this problem, the degree of sophistication ranges from a very sophisticated program for determining the vibrational inputs to an empirical method for determining the distributed aerodynamic loads.

The Function f

The aerodynamic loads were determined by using the methods, tables, and charts from NASA TN D-3283 (Ref. 14) and the aerodynamic inputs from the typical Nitehawk 9 trajectory (Table 2). The aerodynamic loads are shown in Figure 14. The distributed aerodynamic loads are then used as an input into the AEROMOD which determined the body static deflection, the static margin of the vehicle and the aerodynamic moment. These results and the thrust

TABLE 2 Values for Function $f_1(t)$

Time (sec.)	T^* (lb)	u_{3T} (in)	Tu_{3T} (in-lb)	u'_{3T} (in/in)	ℓ_1 (in)	$T^* u'_{3T} \ell_1$ (in-lb)	$T^*(u_{3T} - u_{3T}\ell_1)$ (in-lb)	Aeromon (in-lb)	$T^*(u_{3T} - u'_{3T}\ell_1) - M_{\theta_i}$ (in-lb)
0	10,350	0.04		0.0017	98	1,720	-1310	-26,940	-28,250
.5	8,700	.038	331	.0017	98	1,450	-1120	-24,750	-25,870
.94	970	.033	32	.0017	98	115	- 80	-22,260	-22,340
1.0	0	-	-	-	-	-	-	-21,890	-21,890
1.5	-	-	-	-	-	-	-	-18,050	-18,050
2.0	-	-	-	-	-	-	-	-14,970	-14,970
3.5	-	-	-	-	-	-	-	-10,070	-10,070
4.0	-	-	-	-	-	-	-	- 6,900	- 6,900
5.0	-	-	-	-	-	-	-	- 4,600	- 4,600
6.0	-	-	-	-	-	-	-	- 3,100	- 3,100
7.0	-	-	-	-	-	-	-	- 2,100	- 2,100

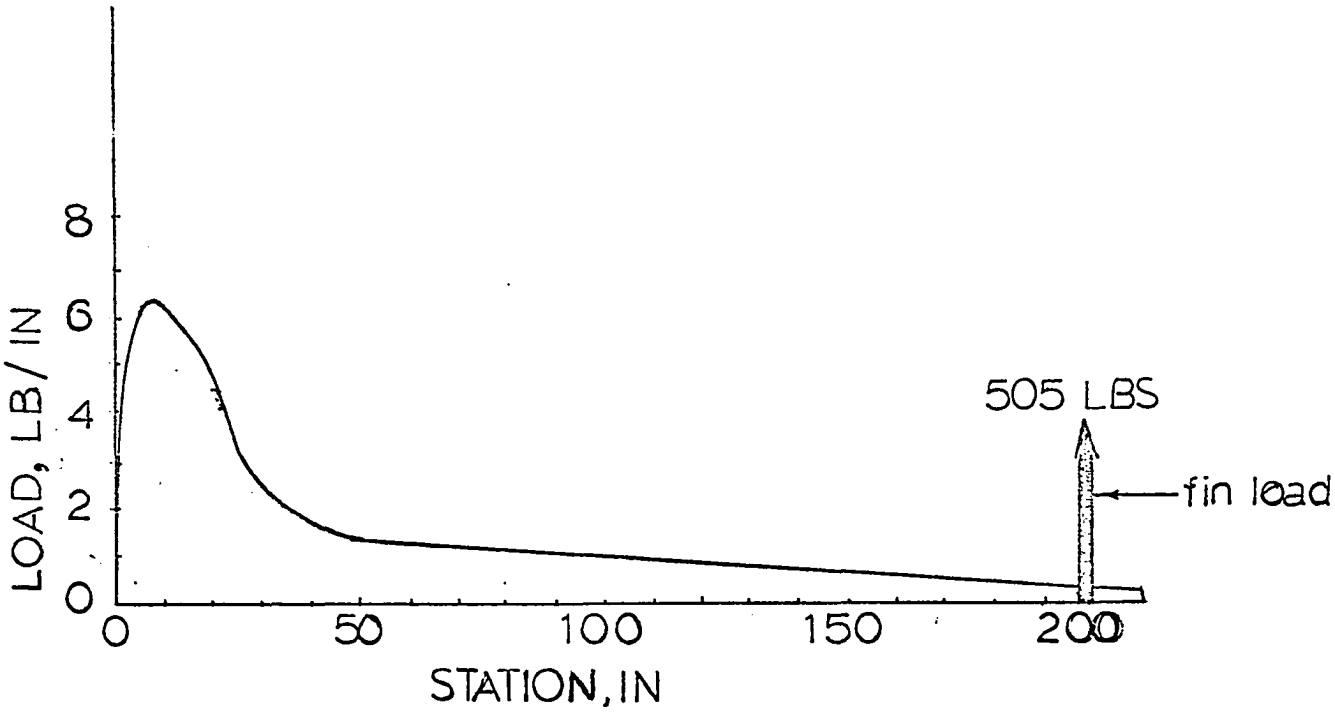

Figure 14

The Aerodynamic Load

force are combined to determine f_1 which is shown in Figure 9. Table 2 shows the numbers used to determine $f_1(t)$.

The Aerodynamic Damping Moment

Davis, Follin, and Blitzer (Ref. 16) defined the aerodynamic damping moment as

$$M_q = -\frac{1}{2} C_m \rho A \ell^2 V\omega = -\frac{1}{2} C_{m_q} \frac{\bar{q}}{V} \ell^2 A \omega \qquad (76)$$

where

C_{m_q} = the damping coefficient, $\bar{q}$ = dynamic pressure, ℓ = reference length, A = reference area, ω = pitch (or yaw) rate ($\dot{r}_2$ or $\dot{r}_3$)

From the work of Curry and Uselton (Ref. 12), the $C_{m_q} = 600$ rad^{-1} for the Nitehawk 9 upper stage at Mach 8. The values calculated for the aerodynamic damping moment are

Time, sec.	M_q, ft-lb.
0.0	892
0.5	780
1.0	665
2.0	456
3.0	298
4.0	210
5.0	140
6.0	96

The aerodynamic damping moment is combined with the jet damping moment to form the function f_2 (see Figure 11.) The roll rate is taken from Ref. 13.

The Jet Damping Moment

From FDL-TDR-64-1 (Pt. 1, V. 1) (Ref. 17), the jet damping force is defined as

$$J_{D_z} = -2\omega \dot{m} X_p$$

where ω = pitching frequency ($\dot{r}_2$ or $\dot{r}_3$), $\dot{m}$ = mass flow rate, X_p = distance from center of mass to the particle of mass. The following moment was calculated for the jet damping force.

Time, sec.	$J_{Dz}\ell$, in - lb
0	89ω
0.5	73ω
0.94	0ω

The jet damping moment is combined with the aerodynamic moment to form the function f_2 (see Figure 10).

Moment Due to Bent Payload

From Reis and Sundberg (Ref. 2), the deflection of the center of mass of the payload from the symetric center line was found to be 0.143 inches. This produces a force of

$$F = mr = 35.5 \text{ lb.}$$

The distance from the center of mass of the system to the center of mass of the payload is 5.5 ft. The resulting moment about the center of mass of the system is

$$M_B = 5.5 \times 35.5 = 195 \text{ ft-lb.}$$

Vibrational Moment

The angular displacement due to vibrational motion was determined by using the Sandia SHOCK Code which is described briefly in Appendix E. The assumption was made that the vibrational motion was induced by the burnout of the propellant in the rocket motor.

The code was used to determine two cases of vibration. In the first case, the vehicle is considered as a continuous beam with mass and moment of inertia varying along its length. In the second case, the vehicle is assumed to have a loose joint at the payload attachment point. This loose joint could have been caused by poor workmanship, failure to tighten the joint, or differential heating of parts caused by aerodynamic heating.

In the first case, the vibrational motion was shown to be near sinusoidal with a constant offset or basis (see Fig. 15). The frequency was shown to be approximately 30 cps or 188 rad/sec.

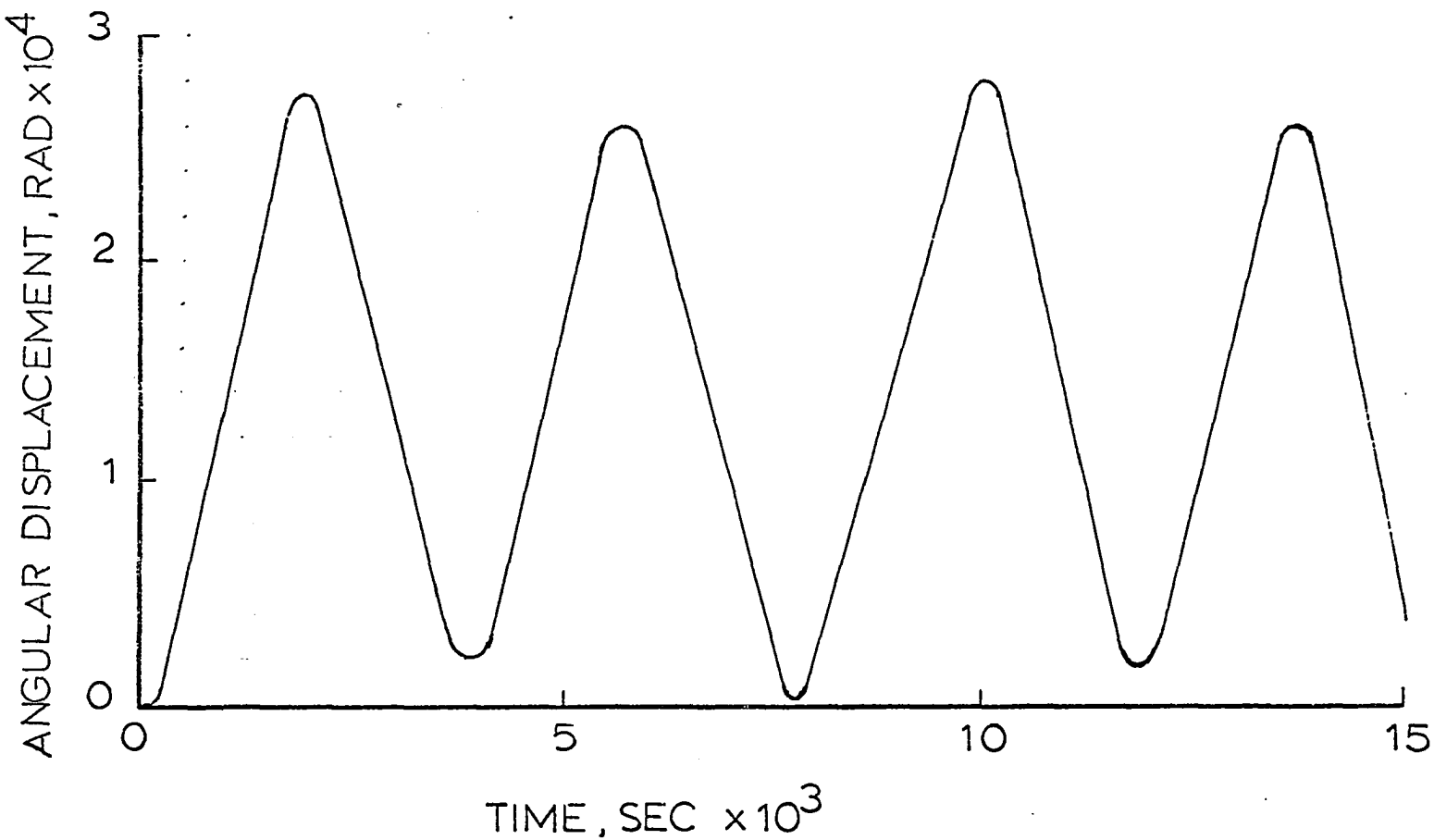

Figure 15 Elastic Vibration

The vibrational motion is for this case equal to (0.0015 + 0.0015 sin 188t) rad. Witte (Ref. 18) showed that the experimental natural frequency of this vehicle was 32 cps.

Witte further showed that the natural frequency of the vehicle could be drastically changed by loosening the separation joint of the payload. Witte was able to change the frequency at will over the range of 2 cps to 32 cps. Reis and Sundberg (Ref. 2) showed that the separation joint could be made loose by differential heating of the joint. The loose joint was shown to have a rotation of 10^{-6} rads/in-lb. Using this rotation, the code gave a vibrational motion of (0.0015 + 0.005 Sin ωt) where ω = 27 rad/sec. (see Fig. 16). This frequency coincided with the steady-state roll rate.

An Arbitrary Moment

Stone (References 4 and 5) showed mathematically the possibility of a highly nonlinear magnus moment as the culprit in the extra-atmosphereic coning motion. Curry and Uselton (Ref. 13) predicted a moment caused by asymmetric lee-side vorticity. At present, there are no coefficients available to estimate the values of these moments. However, since they have gone unnoticed for many years, it should be safe to assume that they are small. For this problem, these moments will be represented by an arbitrary moment of the same magnitude as the moment caused by the bent payload (200 ft-lb).

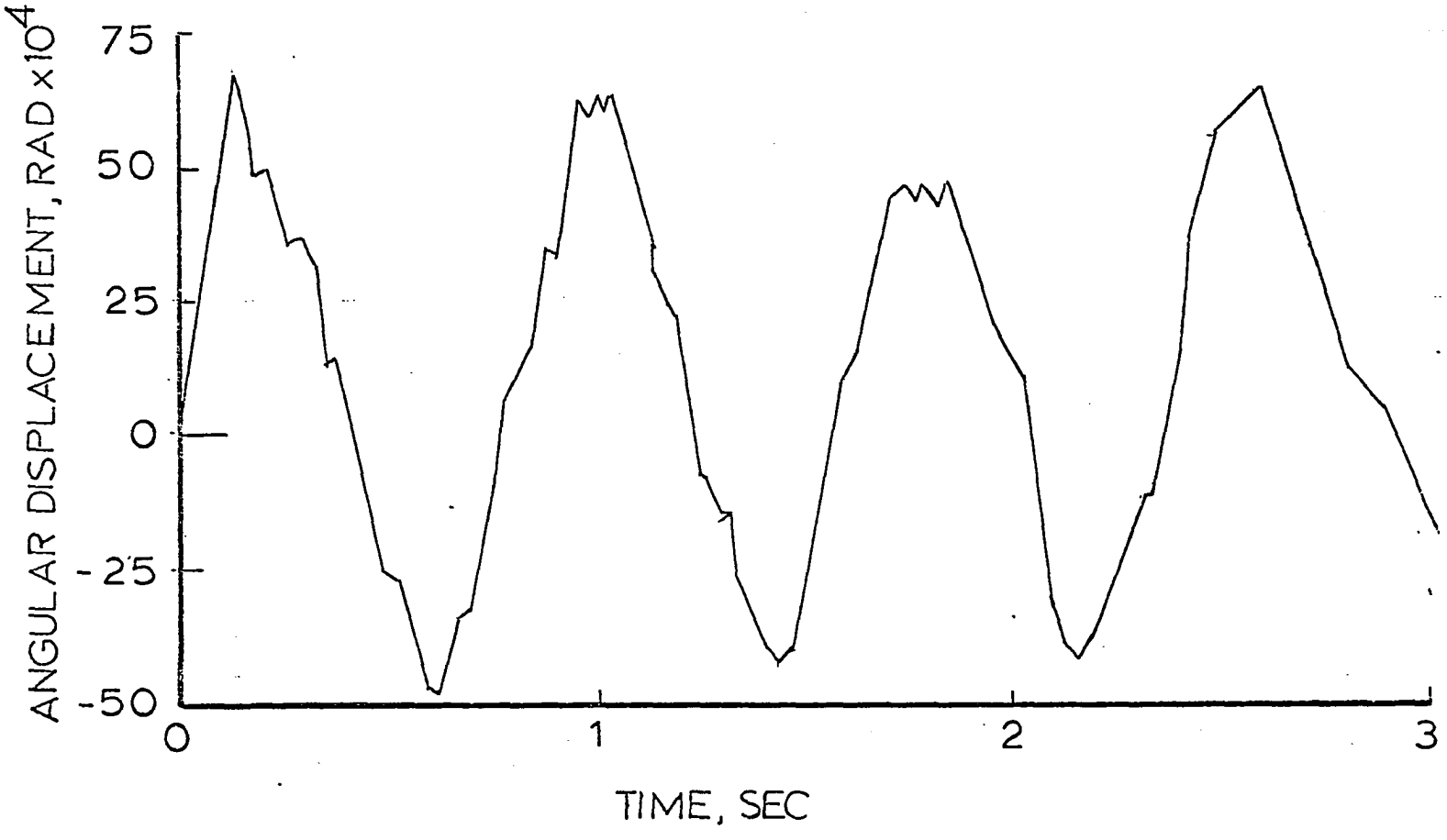

Figure 16 Vibration with Loose Joint

APPENDIX D

THE AEROELASTIC PROGRAM

Aeroelasticity is the study of the effect of aerodynamic forces on elastic bodies (Ref. 19). In most structural problems, it is usually assumed that the deformation is small and does not substantially affect the action of external forces. Even in problems of bending and buckling of columns or plates and shells, either the external loading or the boundary conditions are assumed to be known. In aeroelastic problems, this situation is different. The aerodynamic forces depend entirely on the attitude of the body relative to the flow. The magnitude of the aerodynamic load is not known until the elastic deformation is known. The aerodynamic load is an unknown until the problem is solved.

The computer program which was used to evaluate the aeroelastic properties for the application problem is called AEROMOD. It was written by John C. Weydert, Division 9224, Sandia Laboratories, Albuquerque, New Mexico, and it is a standard tool used in sounding rocket development at Sandia.

To use this program, the following input parameters must be

specified:

Station	Length from zero
Wt/inch	Distributed Structural Weight
Stiffness	$EI/10^6$
Load/inch	Distributed Air Loads
Rotation	Weak or Loose Joint Rotation
Thrust	Motor Thrust
Roll Rate	Rigid-Body Roll Rate
Drag	Drag Force
Dynamic Pressure	Dynamic Pressure
Angle or Attack	Rigid-Body Angle of attack

The program will print out the following information:

Station, Axial Load, Lateral Acceleration, Shear, Bending Moment, Delta Theta, Deflection - Tangent, Deflection, Roll Axis, Local Angle Air Flow, Weight, Total Air Load, Static Margin, Bend Moment at CG, Dynamic Pressure, Angle of Attack, Roll, Torque, Aeromod.

There will be a tabulation of these parameters for the following conditions: Trim Conditions; Elastic Conditions-Converged Shape; Rigid Body Results; Elastic Conditions-Converged Shape; and Roll Conditions-Converged Shape.

```
!EQUIP,72=(36-00003),HI,RO
!EQUIP,16=(36-00531),HI
!COMMENT,SC-4020 TAG FOR LOG. UNIT 16--WEYDERT BX 662,6-BI-HC-CO-SA
!FTN,X,L
      PROGRAM AEROMOD
      DIMENSION AXLO(200),BETA(200),GAMMA(200),TBM(200),H(101)
      DIMENSION W(200),EI(200),RGK(200),ROT(200),XP(200),
     1PR(200),ANG(200),P(200),PSUM(200),
     2G(200),Q(200),BENDMO(200),SHEAR(200),ANGSUM(200),RGKSUM(200)
      DIMENSION DELTHT(200),QSUM(200),VSUM(200),BEI(200),BEISUM(200)
      DIMENSION DELTH(200),PHI(200),ANGOLD(200)
      DIMENSION XLAB1(3),XLAB2(3),XLAB3(3),YLAB(3)
      DIMENSION PT1(4),PT2(4),XLAB4(3)
      DIMENSION TITLE(10)
      COMMON X(200),XDIFF(200),XSUM(200),YBAR(200),WSUM(200),Y(200),
     1DYCG,CG,MAX,PHIAX,PROD
      TYPE REAL IO,IR,ICG
      TYPE INTEGER FLAG,TESTNO
      DATA(XLAB1=8HAXIAL LO,8HADING   ,1H ),
     1(XLAB2=8HBENDING ,8HMOMENT  ,1H ),
     2(XLAB3=8HY DEFLEC,8HTIONS   ,1H ),
     3(YLAB=8HSTATION ,8HPOSITION,1H )
      DATA(XLAB4=8HY DEFLEC,8HTIONS FR,8HOM ROLL )
      DATA(PT1=8H  CONDIT,8HIONS -  ,8HCONVERGE,8HD  SHAPE),
     1(PT2=8HTAIL IS ,8HSTATION ,8H ZERO   ,1H )
      LABXX = 1H*
      THZ = 0.
      THX = 0.
      FX = 0.
      GUST = 0.
      WIND = 0.
      ROLMOM = 0.
      PHIAX = 0.
      GLAT = 0.
      KBINCT=0
      RCON = 57.29578
```

```
      M=1 $ FLAG=0
C     READ IN STRUCTURE DATA
      READ 592,TITLE
592   FORMAT(10A8)
      PRINT 696,TITLE
696   FORMAT(1H1,////,1H0,20X,10A8)
      READ 580,EPS,GAMMAF,DELTA,LIMIT1,LIMIT2
      READ 590,THRUST,THOFF,THMIS,DRAG,OMEGA,GUSTO,DYNP
C***** PROGRAM CONTROL DATA PRINT
      PRINT 6219,EPS,GAMMAF,DELTA,LIMIT1,LIMIT2
6219  FORMAT(1H0,4X,*PROGRAM CONTROL DATA*//
     11H0,4X,*NOSE DEFLECTION CONVERGENCE FACTOR*6X,F10.4/
     21H0,4X,*AFT FIN MISALIGNMENT, DEGREES* 11X,F10.4/
     31H0,4X,*TORQUE CONVERGENCE, INCH POUNDS*9X,F10.4/
     41H0,4X,*DEFLECTION ITERATION LIMIT*14X,I5/
     51H0,4X,*TORQUE ITERATION LIMIT*18X,I5)
580   FORMAT (2F10.3,F10.0,2I5)
590   FORMAT(7F10.0)
      JUMP=0
501   FORMAT(I2,F7.0,6F10.0)
      READ 501,KOMPNUM,X(1),W(1),EI(1),ROT(1),RGK(1),BETA(1),GAMMA(1)
   33 M=M+1
      READ 501,KOMP,X(M),W(M),EI(M),ROT(M),RGK(M),BETA(M),GAMMA(M)
      IF(KOMP.GT.98)GO TO 1
      IF(KOMP.EQ.KOMPNUM)GO TO 2
      STA=X(M-1)
      BASIS=BETA(M-1)
      FLAG=1
      KOMPNUM=KOMP
    4 X(M)=X(M)+STA
      BETA(M)=BASIS+BETA(M)
      GO TO 33
2     IF(FLAG.LT.1)GO TO 33
      GO TO 4
    1 MAX=M-1 $ J=1
C     READ IN DYNAMIC LOAD DATA
```

```
    6 READ 501,M,XP(J),PR(J)
      IF(M.GT.98) GO TO 5
      J=J+1
      GO TO 6
    9 P(J)=((X(J)-XP(I-1))/(XP(I)-XP(I-1)))*(PR(I)-PR(I-1))+PR(I-1)
      LWR=I
      GO TO 8
    5 MAXLIST=J-1
      DO 9170 I = 1,MAX
9170  ROT(I) = ROT(I)*1.E-9
      ANG(1) = 0.
      DO 10 I = 2,MAX
      DELTHT(I)=0
      Y(I) = 0
   10 ANG(I) = ANG(I-1) + BETA(I) + GAMMA(I)
      ATTACK = GAMMAF - 2.*ANG(MAX)
      ANG(1) = ATTACK
      DO 11 I = 2,MAX
      ANG(I) = ANG(I) + ATTACK
   11 ANGSUM(I) = ANG(I) + ANG(I-1)
C-----INTERPOLATE FOR STATION LOADS
      LWR=2
      DO 8 J=1,MAX
      DO 8 I=LWR,MAXLIST
      IF(X(J).GE.XP(I-1).AND.X(J).LE.XP(I)) GO TO 9
    8 CONTINUE
      IF(X(MAX).GT.XP(MAXLIST))PRINT 601
  601 FORMAT(1H0,*----------*2X,*AIR LOADS NOT DEFINED FOR*
     1* ENTIRE VEHICLE*)
      PRINT 668
      PRINT 667,PT2
      PRINT 662,(X(I),W(I),P(I),EI(I),ROT(I),
     1RGK(I),BETA(I),GAMMA(I),I=1,MAX)
      PRINT 690,THRUST,THMIS,THOFF,OMEGA,DRAG
      KONTRL=1
C CALCULATE FIRST + SECOND MOMENTS,WEIGHT,CP,CG
```

```
      DO 295 I=1,MAX
295   ANGOLD(I)=ANG(I)
      DO 200 I=2,MAX
      RGKSUM(I)=RGK(I)+RGK(I-1)
      XSUM(I)=X(I)+X(I-1)
      XDIFF(I)=X(I)-X(I-1)
200   WSUM(I)=W(I)+W(I-1)
3095  CONTINUE
      WT=0
      WM1=0
      IR=0
      IO=0
      DO 201 I=2,MAX
      WT=WT+WSUM(I) *XDIFF(I) *.5
      IO=IO+WSUM(I)*XDIFF(I)*XSUM(I)**2 *0.125
201   IR=IR+RGKSUM(I)*WSUM(I)*XDIFF(I)*.25*1./4626.7
      DO 702 I = 2,MAX
      DO 701 K = 1,11
      FK = K
      H(K) = ((FK - 1.) * (W(I) - W(I-1)) / 10. + W(I-1)) * (X(I-1)
     1+ (FK - 1.) * (X(I) - X(I-1)) / 10.)
701   CONTINUE
      CALL SIMPSON (X(I-1), X(I), 11, H, DELXW)
702   WM1 = WM1 + DELXW
      CG=WM1/WT
      ICG=(IO-WT*CG**2)/4626.7
      JUMBO = 1
309   TESTNO=0
304   CONTINUE
      XAIRLD=0
      AIRLOD=0
      DO 2010 I=2,MAX
      PSUM(I)=P(I)+P(I-1)
      ANGSUM(I)=ANG(I)+ANG(I-1)
      AIRLOD=AIRLOD+PSUM(I)*ANGSUM(I)*XDIFF(I)*0.25
2010  XAIRLD=XAIRLD+PSUM(I)*ANGSUM(I)*XDIFF(I)*XSUM(I)*.125
```

```
C     XAIRLD AND AIRLOD MAY BE ZERO IF TRIM LIMIT=0
      IF(XAIRLD.LT.0.00000001.AND.AIRLOD.LT.0.00000001)GO TO 2029
      CP = XAIRLD/AIRLOD
      GO TO 2028
2029  CP=0
2028  CONTINUE
      IF(KONTRL.LT.2) GO TO 11212
      IF(CP.GE.CG)GO TO 901
11212 CONTINUE
      TORQUE=(CG-CP)*AIRLOD
      AERMOM=TORQUE+THX*DISP-THZ*CG
      TORK = TORQUE
      IF(JUMP.EQ.1)TORQUE=AERMOM
      ABO=RCON*AERMOM/(12.*GUST*ICG)
      IF(KONTRL.EQ.1)ABO=0.
      IF(ABO.LT.0.)ABO=.00000001
      FREQ=1.0/(2.*3.141592)*SQRT(ABO)
      ANGACC=AERMOM/(12.*ICG)
      STMARG=(CG-CP)*100./X(MAX)
      DO 202 I=1,MAX
      GO TO (2000,2001,2001),KONTRL
2000  G(I) = AIRLOD/WT
      GO TO 202
2001  G(I) = (AIRLOD-THZ)/WT - (X(I)-CG)*ANGACC/385.56
     1-Y(I)*OMEGA**2/9.766
202   Q(I)=G(I)*W(I)
C     CALCULATE SHEAR,BENDMO,
C     CALCULATE ROLL MOMENT
      SHEAR(MAX) = 0.
      VSUM(MAX)  = 0.
      BENDMO(MAX)= 0.
      DO 203 I=2,MAX
      QSUM(I)=Q(I)+Q(I-1)
203   CONTINUE
      DO 208 I=2,MAX
208   SHEAR(-I+MAX+1)=SHEAR(-I+MAX+2)+(PSUM(-I+MAX+2)*ANGSUM(-I+MAX+2)
```

```
     1*.25-QSUM(-I+MAX+2)*.5)*XDIFF(-I+MAX+2)
      SHEAR(1) = 20.0 * THZ
      TBM(MAX) = 0
      DO 1000  I=2,MAX
1000  TBM(MAX+1-I) = TBM(MAX+2-I)
     1+ (WSUM(MAX+2-I)*0.5*FX/WT + DRAG/X(MAX))
     2* XDIFF(MAX+2-I)*(Y(MAX+2-I)-Y(MAX+1-I))*0.5
     3+ AXLO(MAX+2-I)*(Y(MAX+2-I)-Y(MAX+1-I))
      DO 204 I=2,MAX
      VSUM(-I+MAX+1)=SHEAR(-I+MAX+2)+SHEAR(-I+MAX+1)
      BENDMO(-I+MAX+1)=BENDMO(-I+MAX+2)+VSUM(-I+MAX+1)
     1*.5*XDIFF(-I+MAX+2) + (TBM(-I+MAX+1)-TBM(-I+MAX+2))
204   CONTINUE
      DO 335 I = 1,MAX
  335 BEI (I) = BENDMO(I) / EI(I)
      DO 336 I = 2,MAX
  336 BEISUM(I) = BEI(I) + BEI(I-1)
      DELTHT(1) = 0
      DO 205 I=2,MAX
      DELTHT(I) = DELTHT(I-1) + BEISUM(I) * XDIFF(I) * 0.50
     1* 1.E-6 * RCON + BENDMO(I) * ROT(I) * RCON
205   CONTINUE
      DO 206 I=1,MAX
206   DELTHT(I)=DELTHT(MAX)-DELTHT(I)
      SAVE = ANG(MAX)
      DO 300 I=1,MAX
300   ANG(I)=ANGOLD(I)-DELTHT(I)
C-----CALCULATE DEFLECTIONS FROM CG
      J=2
211   IF(X(J).GT.CG)GO TO 220
      KEEP=J
      J=J+1
      GO TO 211
220   DELTCG=((CG-X(J-1))/(X(J)-X(J-1)))*(DELTHT(J)-DELTHT(J-1))
     1+DELTHT(J-1)
      ANGCG=((CG-X(J-1))/(X(J)-X(J-1)))*(ANG(J)-ANG(J-1))
```

```
     1+ANG(J-1)
      EICG  =((CG-X(J-1))/(X(J)-X(J-1)))*(EI(J)-EI(J-1))    +EI(J-1)
      BENDCG=((CG-X(J-1))/(X(J)-X(J-1)))*(BENDMO(J)-BENDMO(J-1))
     1 + BENDMO(J-1)
      VECTOR=WIND-ANGCG
      IF(KONTRL .EQ. 1) GO TO 83
      DO 3003 I=1,MAX
3003  ANG(I) = ANG(I) + VECTOR - PHIAX
   83 CONTINUE
      DO 210 I=1,MAX
      N=0
      IF(X(I).GT.CG)N=1
210   PHI(I)=(DELTHT(I) - BETA(I) - DELTCG)*(-1)**N
      KEP=KEEP+1
      KEP1=KEP+1
C-----FOR STATIONS FORWARD OF CG
      T = 1.E-6*BEI(KEP)*(X(KEP)-CG)**2*.333333
     1+ 1.E-6*BENDCG/EICG*(X(KEP)-CG)**2*.166667
      YBAR(KEP) = T
      DO 324 I=KEP1,MAX
      DIN = PHI(I-1)/RCON*XDIFF(I)
      T = 1.E-6*BEISUM(I)*XDIFF(I)**2*.166667
     1+ 1.E-6*BEI(I)*XDIFF(I)**2*.166667
324   YBAR(I) = YBAR(I-1) + DIN + T
C-----FOR STATIONS AFT OF CG
      T = 1.E-6*BEI(KEEP)*(CG-X(KEEP))**2*.333333
     1+ 1.E-6*BENDCG/EICG*(CG-X(KEEP))**2*.166667
      YBAR(KEEP) = T
      DO 3241 I=2,KEEP
      J = KEP - I
      DIN = PHI(J+1)/RCON*XDIFF(J+1)
      T = 1.E-6*BEISUM(J+1)*XDIFF(J+1)**2*.166667
     1+ 1.E-6*BEI(J)*XDIFF(J+1)**2*.166667
3241  YBAR(J) = YBAR(J+1) + DIN +T
      IF(KONTRL.EQ.2.AND.TESTNO.EQ.0)GO TO 306
 5002 CONTINUE
```

```
      TESTNO=TESTNO+1
      IF(ABS(ANG(MAX)-SAVE).LE.ABS(ANG(MAX)*EPS))GO TO 250
302   IF(TESTNO.GT.LIMIT1)GO TO 260
3040  IF(JUMP.EQ.1)GO TO 310
      GO TO 304
250   GO TO (314,306,306),KONTRL
260   GO TO (303,261,261),KONTRL
303   PRINT 618,ATTACK,TORQUE,TESTNO,LABXX
      PRINT 621
      CALL EXIT
261   PRINT 618,DELTHT(1),DYCG,TESTNO
      CALL EXIT
3060  FLAG = 1
      GO TO 306
314   IF(ABS(TORQUE).LE.DELTA)GO TO 3060
      KBINCT = KBINCT + 1
      IF(KBINCT.GT.LIMIT2)GO TO 303
      IF(JUMBO.GT.1)GO TO 402
400   CHANGE = 0.10
401   ATTACK = ATTACK + CHANGE
      DO 308 I=1,MAX
      ANGOLD(I) = ANGOLD(I) + CHANGE
308   ANG(I) = ANG(I) + CHANGE
      STORQUE = TORQUE
      JUMBO = JUMBO + 1
      GO TO 309
402   RATE = (STORQUE - TORQUE)/CHANGE
      CHANGE = TORQUE/RATE
      ATTACK = ATTACK + CHANGE
      DO 399 I=1,MAX
      ANGOLD(I) = ANGOLD(I) + CHANGE
399   ANG(I) = ANG(I) + CHANGE
      JUMBO = 1
      GO TO 309
C     309 INDICATES NEW RUN (TESTNO=0 AGAIN)
307   PRINT 617
```

```
306   CONTINUE
C     OUTPUT REGULAR RESULTS
      PRINT 692
692   FORMAT(1H1,//////////)
      GO TO(3220,3221,3222),KONTRL
3220  PRINT 664,PT1
      GO TO 3223
3221  PRINT 665,PT1
      GO TO 3223
3222  PRINT 666,PT1
3223  CONTINUE
      IF(KONTRL.EQ.2.AND.TESTNO.EQ.0)GO TO 5001
5003  CONTINUE
      PRINT 661,WT,CG,AIRLOD,CP,STMARG,ICG,FREQ,
     1ROLMOM,BENDCG,DELTHT(1),DYNP,THRUST,GUSTO,DRAG,OMEGA,
     2TORK,AERMOM,TBM(1),THX,THZ,FX,DYCG,PHIAX,PROD
      PRINT 669
      PRINT 667,PT2
      PRINT 663,(X(I),AXLO(I),G(I),SHEAR(I),BENDMO(I),
     1DELTHT(I),YBAR(I),Y(I),ANG(I),I=1,MAX)
      IF(KONTRL.EQ.2.AND.TESTNO.EQ.0)GO TO 5002
      IF(KONTRL.EQ.1)GO TO 5004
5005  CONTINUE
      IF(JUMP.EQ.1)GO TO 11125
      GUST=GUSTO
      IF(FLAG)310,310,311
5001  PRINT 670
670   FORMAT(1H0,50X,*RIGID BODY RESULTS*)
      GO TO 5003
5004  PRINT 693,ATTACK
693   FORMAT(1H0,25X,*TRIM ANGLE  =*,F12.8)
      GO TO 5005
311   DO 312 I=1,MAX
      ANGOLD(I)=ANG(I)+GUST
312   ANG(I)=ANG(I)+GUST
      SAVE = ANG(MAX)
```

```
      WIND=ATTACK+GUST-DELTCG
      FLAG = 0
      KONTRL=2
      GO TO 309
310   CONTINUE
      WM2 = 0
      DO 325 I = 2,MAX
325   WM2 = WM2 + WSUM(I) * XDIFF(I) * (YBAR(I) +
     1YBAR(I-1))/4.
      DYCG = WM2/WT
      CALL ROLLAX
320   CONTINUE
      PHIAX=PHIAX*RCON
      JUMP=1
      PHITR=DELTHT(1)+BETA(1)+THMIS+PHIAX-DELTCG
      THX=THRUST*COS(PHITR/RCON)
      THZ=THRUST*SINF(PHITR/RCON)
      FX=THX-DRAG
      AXLO(1) = THX
      DO 330  I = 2,MAX
330   AXLO(I)=AXLO(I-1)-(DRAG/X(MAX))*XDIFF(I)
     1-(FX/WT)*WSUM(I)*XDIFF(I)* 0.5
      DISP=THOFF+Y(1)
      KONTRL=3
      GO TO 304
11125 CONTINUE
      CALL ENTFLM                                                    C
      CALL KWKPLT(X,BENDMO,MAX,YLAB,XLAB2)                           C
      CALL KWKPLT(X,Y,MAX,YLAB,XLAB4)                                C
      CALL KWKPLT(X,AXLO,MAX,YLAB,XLAB1)                             C
      CALL EXTFLM                                                    C
      CALL EXIT
  617 FORMAT(*0VEHICLE UNSTABLE OR TRIM ANGLE OUTSIDE OF SEARCH *    ARTM144
     1  *INTERVAL.*)                                                ARTM145
  621 FORMAT(*0*/*0*,54X,*NO TRIM ANGLE FOUND.*)                     ARTM156
901   PRINT 610
```

```
  618 FORMAT(E13.5,E15.5,I6,A1,* ATTEMPT TO ITERATE BEYOND LIMIT.  NO*  ARTM146
     1  * CONVERGENCE.*)                                               ARTM147
 610  FORMAT(1H0,8H********,10X,*PROGRAM TERMINATED*,8X,*DYNAMICALLY *,
     1*UNSTABLE*)
      CALL EXIT
 690  FORMAT(1H0,*  THRUST     =*,F20.10/1H ,
     1*  THRUST MISALIGNMENT     =*,F20.10/1H ,
     2*  THRUST OFFSET     =*,F20.10/1H ,
     3*  ROLL RATE     =*,F20.10/1H ,*  DRAG     =*,F20.10///)
 662  FORMAT(*0STATION*3X*WT/INCH*3X*LOAD/INCH*3X,
     18HEI/10**6,5X*ROTATION*4X*GYRATION*5X*BETA*8X
     2*GAMMA*/1H0,2X*INCHES*5X*LBS*8X*LBS*5X*LB IN SQ*
     35X*RAD IN LB*4X*INCHES*6X*DEGREES*6X*DEGREES*//
     44(1H ,F7.2,4X,F6.2,4X,F7.2,3X,F9.2,3X,4(E10.3,2X)))
 663  FORMAT(*0STATION*3X*AXIAL LOAD*3X*LAT ACCEL*4X,
     1*SHEAR*4X*BENDING MOMENT*4X*DELTA THETA*4X
     2*DEFLECTION*4X*DEFLECTION*4X*LOCAL ANGLE*/1H ,
     378X*CG TANGENT*5X*ROLL AXIS*5X*AIR FLOW*/1H0,1X*INCHES*6X
     4*LBS*5X*FT/SEC SQ/32.13*2X*LBS*6X*INCH LBS*10X
     5*DEGREES*8X*INCHES*8X*INCHES*7X*DEGREES*// (1H ,F7.2,
     63X,F8.0,5X,F7.2,4X,F8.0,4X,F9.0,11X,F6.3,7X,F7.3,
     77X,F7.3,8X,F6.3))
 664  FORMAT(1H0,50X,*TRIM*,4A8)
 665  FORMAT(1H0,46X,*ELASTIC*,4A8)
 666  FORMAT(1H0,50X,*ROLL*,4A8)
 667  FORMAT(1H0,   1H ,49X,4A8,/)
 668  FORMAT(1H1,53X,*INPUT DATA*/1H0,46X,
     1*STRUCTURAL   AND   AIRLOAD*//)
 669  FORMAT(1H1,44X,*OUTPUT  DATA  PER  *
     1*STATION  POSITION*//)
 661  FORMAT(1H0,4X,*WEIGHT*15X*LBS*16X,F10.0,1H.,9X,
     1*CG LOCATION*10X*INCHES*14X,F12.2/
     21H0,4X,*TOTAL AIRLOAD*8X*LBS*16X,F10.0,1H.,9X,
     3*CP LOCATION*10X*INCHES*14X,F12.2/
     41H0,4X,*STATIC MARGIN*8X*PERCENT LENGTH*6X,F12.2,7X,
     5*PITCH INERTIA*8X*SLUG FT SQ*10X,F12.2/
```

```
     61H0,4X,*PITCH FREQUENCY*6X*CYCLES/SEC*10X,F12.2,7X,
     7*ROLL INERTIA*9X*SLUG FT SQ*10X,F12.2/
     81H0,4X,*BEND MOMENT AT CG*4X*INCH LBS*11X,F10.0,1H.,9X,
     9*TOTAL DEFLECTION*5X*DEGREES*13X,F12.2/
     11H0,4X,*DYNAMIC PRESSURE*5X*LBS/FT SQ*10X,F10.0,1H.,9X,
     2*THRUST*15X*LBS*16X,F10.0,1H.,/
     31H0,4X,*ANGLE OF ATTACK*6X*DEGREES*13X,F12.2,7X,
     4*DRAG*17X*LBS*16X,F10.0,1H.,/
     51H0,4X,*ROLL*17X*CYCLES/SEC*10X,F12.2/
     61H0,4X,*TORQUE*15X*INCH LBS*11X,F10.0,1H./
     71H0,4X,*AERMOM*15X*INCH LBS*11X,F10.0,1H./
     81H0,4X,*TBM(1)*15X*INCH LBS*11X,F10.0,1H./
     91H0,4X,*THX*18X*LBS*16X,F10.0,1H./
     11H0,4X,*THZ*18X*LBS*16X,F10.0,1H./
     21H0,4X,*FX*19X*LBS*16X, F10.0,1H./
     31H0,4X,*DYCG*17X*INCHES*14X,F15.5/
     41H0,4X,*PHIAX*16X*DEGREES*13X,F15.5/
     51H0,4X,*PROD*17X*LB INCH SQ*10X,F12.2)
      END
      SUBROUTINE ROLLAX
      DIMENSION YSUM(200)
      COMMON X(200),XDIFF(200),XSUM(200),YBAR(200),WSUM(200),Y(200),
     1DYCG,CG,MAX,PHIAX,PROD
      JUMBO = 1
      PHIAX = 0
10    CONTINUE
      PROD = 0
      DO 1 I=1,MAX
1     Y(I) = YBAR(I) - DYCG + PHIAX * (CG-X(I))
      DO 2 I=2,MAX
      YSUM(I) = Y(I) + Y(I-1)
2     PROD = PROD + WSUM(I)*XDIFF(I)*YSUM(I)*(XSUM(I)*.5-CG)*0.25
      GO TO (20,30,40),JUMBO
20    IF (ABS(PROD).LE.(1.0)) GO TO 40
      SPROD = PROD
      JUMBO = JUMBO + 1
      PHIAX = .005
```

```
      GO TO 10
30    PHIAX = -PHIAX * SPROD/(PROD - SPROD)
      JUMBO = JUMBO + 1
      GO TO 10
40    RETURN
      END
      SUBROUTINE SIMPSON ( XI, XF,  N, H, AREA)
      DIMENSION H(101)
      FN = N
      DELX =(XF - XI) /(FN - 1.)
    1 SUM = 0.
    2 K = (N-1 ) / 2
    3 DO 4 I = 1,K
    4 SUM = SUM + 4. * H(2*I) + 2.*H(2*I-1 )
    6 SUM = SUM - H(1) + H(N)
    8 AREA = (DELX/3.) * SUM
   10 RETURN
      END
         SCOPE
! LIBRARY,72
! LOAD
! RUN,5,3000
NIKE-TOMAHAWK 9      T=20 SEC  M=7.85     Q=7780 PSF      WOMACK
       .002      0.0       50.       50   50
     10305.      0.000       .000      1240.       0.0        1.00      7783.
10    0.        0.00       800.
10    1.         .60       800.
10    5.        3.00       720.
10    9.       18.00       800.
10   10.       18.00       800.
10   11.        2.00       800.
10   15.        2.00       800.
10   16.        0.40       312.
10   20.        0.40       312.
10   25.        0.40       312.
10   30.        0.40       312.
```

10	35.	0.40	312.
10	40.	0.40	312.
10	45.	0.40	312.
10	50.	0.40	312.
10	55.	0.40	312.
10	60.	0.40	312.
10	65.	0.40	312.
10	70.	0.40	312.
10	75.	0.40	312.
10	80.	0.40	312.
10	85.	0.40	312.
10	90.	0.40	312.
10	95.	0.40	312.
10	100.	0.40	312.
10	105.	0.40	312.
10	110.	0.40	312.
10	115.	0.40	312.
10	120.	0.40	312.
10	125.	0.40	312.
10	130.	0.40	312.
10	135.	0.40	312.
10	136.	0.60	800.
10	140.	0.60	700.
10	141.	1.00	200.
10	145.	1.00	200.
10	146.	10.00	200.
10	150.	10.00	200.
10	151.	0.65	200.
10	151.	0.65	200.
10	155.	0.65	200.
10	156.	0.65	200.
10	160.	0.65	200.
10	161.	10.00	200.
10	162.	5.00	200.
10	163.	0.65	200.
10	165.	0.65	200.

```
10 170.      0.65      200.
10 175.      0.65      200.
10 180.      0.65      200.
10 183.      0.65      200.
10 184.     12.00      200.
10 185.     12.00      200.
10 186.      0.80      200.
10 189.      2.56      200.
10 190.      0.75      200.
10 192.      0.69      200.
10 195.      0.60      200.
10 198.      0.54      200.
10 200.      0.50      200.
10 202.      0.46      200.
10 205.      0.40      200.
10 208.      0.16       82.
10 210.      0.00       00.
99
     0.       0.0
     1.        .72
     9.        .72
    10.     505.
    11.        .72
    15.        .72
   140.        .72
   150.        .80
   160.       1.12
   170.       1.70
   180.       2.38
   183.       2.63
   184.       3.74
   186.       4.61
   189.       5.45
   192.       6.25
   195.       6.71
   198.       6.62
```

```
   202.        5.96
   205.        4.55
   208.        2.85
   210.        0.0
71 05 21
71 05 21
```

BINARY * *
BINARY * *

APPENDIX E

THE SHOCK CODE

The SHOCK code calculates the dynamic response of a structure modeled as a spring-mass system having one or two degrees of freedom for each mass when subjected to specified environments. The code determines the behavior of each lumped mass (displacement, velocity, and acceleration for each degree of freedom) and the behavior of each spring or coupling (force, shear, moment, and displacement) as a function of time.

The user has a large number of options for defining the environment for a given problem. The options for describing the load environments include transient conditions such as shock, blast, initial velocities, and initial displacements. Also included are options for describing steady-state loads, preloads, axial g-loads, and maneuver loads.

Some of the more convenient features of the code include the plotting of mass and spring behavior as a function of time; output of minimum and maximum values of accelerations, forces, shears, and moments; output of a data input list with initial conditions; edits

of dynamic response of all springs and masses at user-defined increments; and ease of input. All standard input cards are read using the same format, and, except for a few cases, are independent of order. A complete description of this program is given in Ref. 20.

APPENDIX F

THE ANALOG COMPUTER CIRCUIT

The analog computer used in this dissertation is an Electronic Associates, Inc. Model EAI-680. It is a fully expanded, solid state, 10-volt computer with logic and digital capability. The analog computer circuit is shown in Figure 17.

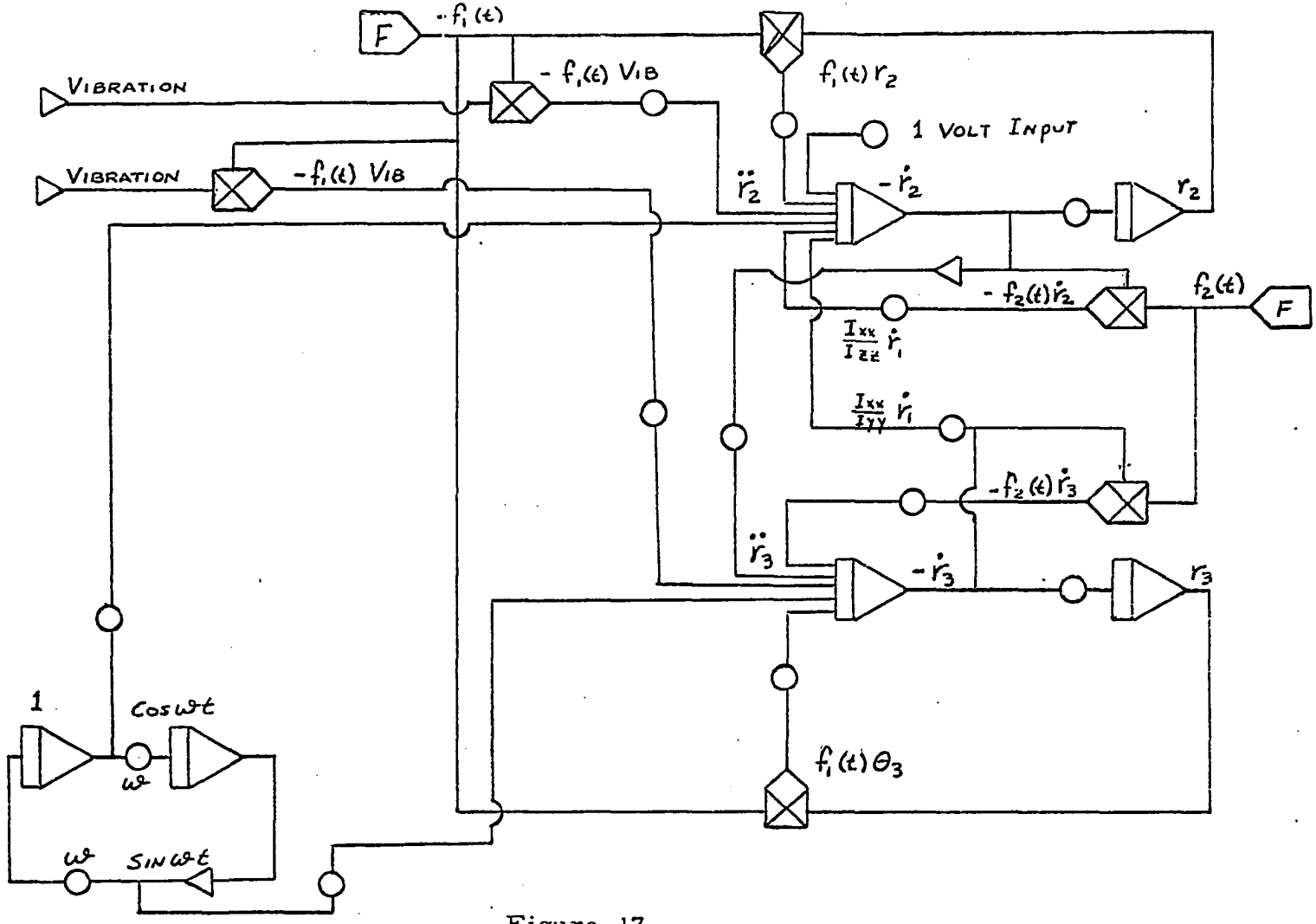

Figure 17

The Analog Computer Circuit